Numerische Mathematik (2020) 146:51–104
https://doi.org/10.1007/s00211-020-01140-0

Numerische Mathematik

Optimization of the shape of regions supporting boundary conditions

Charles Dapogny[1] · **Nicolas Lebbe**[2] · **Edouard Oudet**[1]

Received: 11 March 2019 / Revised: 11 June 2020 / Published online: 12 August 2020

Abstract
This article deals with the optimization of the shape of the regions assigned to different types of boundary conditions in the definition of a 'physical' partial differential equation. At first, we analyze a model situation involving the solution u_Ω to a Laplace equation in a domain Ω; the boundary $\partial\Omega$ is divided into three parts Γ_D, Γ and Γ_N, supporting respectively homogeneous Dirichlet, homogeneous Neumann and inhomogeneous Neumann boundary conditions. The shape derivative $J'(\Omega)(\theta)$ of a general objective function $J(\Omega)$ of the domain is calculated in the framework of Hadamard's method when the considered deformations θ are allowed to modify the geometry of Γ_D, Γ and Γ_N (i.e. θ does not vanish on the boundary of these regions). The structure of this shape derivative turns out to depend very much on the regularity of u_Ω near the boundaries of the regions Γ_D, Γ and Γ_N. For this reason, in particular, $J'(\Omega)$ is difficult to calculate and to evaluate numerically when the transition $\overline{\Gamma_D} \cap \overline{\Gamma}$ between homogeneous Dirichlet and homogeneous Neumann boundary conditions is subject to optimization. To overcome this difficulty, an approximation method is proposed, in which the considered 'exact' Laplace equation with mixed boundary conditions is replaced with a 'smoothed' version, featuring Robin boundary conditions on the whole boundary $\partial\Omega$ with coefficients depending on a small parameter ε. We prove the consistency of this approach in our model context: the approximate objective function $J_\varepsilon(\Omega)$ and its shape derivative converge to their exact counterparts as ε vanishes. Although it is rigorously justified only in a model problem, this approximation methodology may be adapted to many more complex situations, for example in three space dimensions, or in the context of the linearized elasticity system. Various numerical examples are eventually presented in order to appraise the efficiency of the proposed approximation process.

Mathematics Subject Classification 49Q10 · 65K05 · 35B65 · 49M41

Extended author information available on the last page of the article

1 Introduction

Stimulated by the multiple prospects offered by fields so diverse as structural engineering, fluid mechanics, electromagnetism or biology, to name a few, shape and topology optimization techniques have aroused much enthusiasm in the scientific and industrial communities; see for instance [6,12,31,45] for reference monographs, and [22,34] for an account of recent developments and research perspectives.

Shape optimization problems consist in minimizing a given objective function $J(\Omega)$ of the domain Ω, possibly under some constraints. In most realistic applications, $J(\Omega)$ depends on the optimized shape Ω via a *state* u_Ω arising as the solution to a boundary value problem for a certain partial differential equation posed on Ω, which characterizes its physical situation.

Quite often, it turns out that only one part of the boundary $\partial\Omega$ of the shape is subject to optimization, which is associated to one single type of boundary conditions for the state u_Ω in the underlying physical partial differential equation, while the remaining regions are not meant to be modified. For example, in structural design, where u_Ω is the displacement of the structure and is the solution to the linearized elasticity system, it is customary to optimize only the traction-free part of $\partial\Omega$ (i.e. that bearing homogeneous Neumann boundary conditions). Likewise, in fluid applications (where u_Ω is the velocity of the fluid, solution to the Stokes or Navier-Stokes equations), one is often interested in optimizing only the region of $\partial\Omega$ supporting no-slip (that is, homogeneous Dirichlet) boundary conditions.

A little surprisingly, the dependence of a given performance criterion $J(\Omega)$ with respect to the relative locations of regions accounting for different types of boundary conditions has been relatively seldom investigated in shape and topology optimization. Yet, situations where it is desirable to optimize not only the overall shape of Ω but also the repartition of the zones on $\partial\Omega$ bearing different types of boundary conditions are multiple in concrete applications. Let us mention a few of them:

- When the objective criterion involves thermal effects inside the optimized shape Ω, u_Ω is the temperature, solution to the stationary heat equation. The regions of $\partial\Omega$ associated to Dirichlet boundary conditions are those where a known temperature profile is imposed, while Neumann boundary conditions account for heat injection. It may be desirable to investigate the regions where heat should enter the medium Ω (or those which should be kept at fixed temperature) in order to minimize, for instance, the mean temperature inside Ω, or its variance; see for instance [10] about such physical applications.
- In the context of linearly elastic structures, (homogeneous) Dirichlet boundary conditions account for the regions of $\partial\Omega$ where the structure is fixed, while inhomogeneous (resp. homogeneous) Neumann boundary conditions correspond to regions of $\partial\Omega$ where external loads are applied (resp. to traction-free regions). It may be of great interest to optimize the design of fixations [49], or the places where loads should be applied. One interesting application of this idea concerns the optimization of a clamping-locator fixture system (a very brief outline of the stakes of this subject is provided in Sect. 5.2 below); see for instance [41] in the framework of density-based topology optimization methods, or the contributions

[36,50], relying on genetic algorithms or artificial neural networks. More recently, in [56,57] the authors present an adapted level set method for the joint optimization of the shape of an elastic structure Ω and of the region of its boundary $\partial\Omega$ where it should be fixed; see also [58] for analogous simultaneous optimization problems of the structural shape and of the support region using parametrized level set functions and B-spline finite element methods.

– In acoustic applications, u_Ω is the solution to the time-harmonic Helmholtz equation. In this situation, the contribution [24] deals with the optimal repartition of an absorbing material (accounted for by Robin-like boundary conditions) on the walls of a room in order to minimize the sound pressure.

From the mathematical point of view, the above problems are of unequal difficulty: the calculation of the shape derivative $J'(\Omega)$ of the optimized criterion $J(\Omega)$ (or that of the constraint functions) in the framework of Hadamard's method depends very much on the regularity of the physical state u_Ω of the problem in the neighborhood of the optimized transition region between zones bearing different types of boundary conditions. In some of the above situations, u_Ω is 'smooth enough' near these transitions, and the calculation of $J'(\Omega)$ is achieved by classical means. On the contrary, the situation become much more difficult to analyze when u_Ω happens to be 'weakly singular' near these transitions; indeed, the calculation of the shape derivative of $J(\Omega)$ requires a precise knowledge of this singular behavior of u_Ω. The resulting formula is also quite difficult to handle in algorithmic practice, since it brings into play quantities which somehow measure this singular behavior, that are difficult to evaluate from the numerical viewpoint. To the best of our knowledge, the first theoretical calculation of shape derivatives in a context where regions bearing different types of boundary conditions are optimized—dealing with the difficulty of a 'weakly singular' state u_Ω—dates back to [28]. Such calculations have also been considered in a series of articles [8,47] by the so-called Generalized J-integral method. The authors of the latter references propose a mesh refinement procedure in order to achieve an accurate numerical calculation of the state function in the neighborhood of the transition between regions of $\partial\Omega$ with different boundary conditions.

Our purpose in this article is to study such shape optimization problems in which the regions of the boundary of the optimized shape Ω bearing different types of boundary conditions are subject to optimization. Most of the theoretical analysis unfolds in a model two-dimensional situation where a functional $J(\Omega)$ of the shape Ω is minimized; $J(\Omega)$ depends on Ω via a state u_Ω which is the solution to a Laplace equation with mixed boundary conditions: the boundary $\partial\Omega$ is divided into three regions Γ_D, Γ_N and Γ, and u_Ω satisfies homogeneous Dirichlet boundary conditions on Γ_D, inhomogeneous Neumann boundary conditions on Γ_N, and homogeneous Neumann boundary conditions on Γ; see (2.2) below. At first, we rigorously calculate the derivative $J'(\Omega)$ of $J(\Omega)$ with respect to variations of the shape Ω in both situations where the transitions $\Sigma_N = \overline{\Gamma} \cap \overline{\Gamma_N}$ and $\Sigma_D = \overline{\Gamma} \cap \overline{\Gamma_D}$ are also subject to optimization. In the former case, the shape derivative turns out to have a classical structure, and it lends itself to a fairly simple treatment in numerical algorithms. On the contrary, in the latter context, the state u_Ω is weakly singular near Σ_D, which makes the formula for $J'(\Omega)$ uneasy to handle in practice. To circumvent this drawback, our second contribution is to propose

an approximation method for the considered state problem (2.2), and thereby for the resulting shape optimization problem: elaborating on the idea developped in [24] and on our previous work [4], the considered 'exact' Laplace equation with mixed boundary conditions is replaced with an approximate counterpart, parametrized by a 'small' parameter ε, where Robin boundary conditions with ε-varying coefficients are imposed on the whole boundary $\partial\Omega$: the 'sharp' transition Σ_D between regions equipped with homogeneous Dirichlet and Neumann boundary conditions is thus 'smeared' into a zone with thickness ε; the shape optimization problem of the counterpart $J_\varepsilon(\Omega)$ of $J(\Omega)$ where u_Ω is replaced with the approximate state $u_{\Omega,\varepsilon}$ lends itself to an easier mathematical analysis: in particular, the approximate shape derivative $J'_\varepsilon(\Omega)$ does not involve any singular component, and it is therefore much easier to use in practice. We then turn to prove the consistency of this approach: namely, the approximate objective function $J_\varepsilon(\Omega)$ and its shape derivative $J'_\varepsilon(\Omega)$ converge to their exact counterparts $J(\Omega)$ and $J'(\Omega)$ when the smoothing parameter ε vanishes.

Let us emphasize that although this approximation method is rigorously justified only in a model situation, it is easy to generalize (and thus to use in a formal way) to many different, more involved situations, such as that of the linearized elasticity system (in two or three space dimensions), and we discuss several numerical examples in this spirit.

The remainder of this article is organized as follows. In Sect. 2, we present the considered model situation, involving the solution u_Ω to a Laplace equation with mixed boundary conditions, and we recall some 'classical', albeit technical material about the regularity of the state function u_Ω in the neighborhood of the transition between regions associated to different types of boundary conditions. In Sect. 3, we carefully calculate the shape derivative of a generic objective functional $J(\Omega)$ of the domain involving u_Ω in both contexts where the transitions Σ_N and Σ_D between, respectively, inhomogeneous Neumann–homogeneous Neumann and homogeneous Dirichlet–homogeneous Neumann boundary conditions are also subject to optimization. In Sect. 4, we focus on the second situation, which turns out to be especially intricate. We propose an approximation of the considered state problem which makes it much easier to analyze from the theoretical viewpoint, and supplies an approximate version $J_\varepsilon(\Omega)$ of $J(\Omega)$ which is quite convenient to use in numerical practice (in particular, its shape derivative is easier to evaluate); we then prove the consistency of this approximation process. The efficiency of the methods proposed in this article is illustrated in Sect. 5: model, analytical test-cases are investigated as well as more realistic applications such as optimization examples of 3d elastic structures. This article ends with the technical Appendix A in which some useful facts about tangential calculus are recalled.

2 Optimization of a function of the domain allowing variations of the regions supporting boundary conditions

In this section, we present the model problem under scrutiny in most of the article, which concentrates the main difficulties we plan to address in a simplified setting, and lends itself to a rather complete mathematical analysis.

2.1 Presentation of the model physical problem and notations

Let $\Omega \subset \mathbb{R}^d$ be a smooth bounded domain ($d = 2$ or 3 in applications), whose boundary $\partial\Omega$ is divided into three disjoint, complementary open regions $\Gamma_D \neq \emptyset$, Γ_N and Γ:

$$\partial\Omega = \overline{\Gamma_D} \cup \overline{\Gamma_N} \cup \overline{\Gamma}. \tag{2.1}$$

We denote by u_Ω the unique solution in the space

$$H^1_{\Gamma_D}(\Omega) := \left\{ u \in H^1(\Omega),\ \ u = 0 \text{ on } \Gamma_D \right\}$$

to the following mixed boundary value problem:

$$\begin{cases} -\Delta u_\Omega = f \text{ in } \Omega, \\ u_\Omega = 0 \quad \text{on } \Gamma_D, \\ \frac{\partial u_\Omega}{\partial n} = g \quad \text{on } \Gamma_N, \\ \frac{\partial u_\Omega}{\partial n} = 0 \quad \text{on } \Gamma, \end{cases} \tag{2.2}$$

where n is the unit normal vector to $\partial\Omega$, pointing outward Ω, and the source term f and boundary flux g are supposed to be regular enough, say $f \in L^2(\mathbb{R}^d)$, $g \in H^1(\mathbb{R}^d)$. Note that g may vanish on some subset of Γ_N, so that the inclusion $\Gamma \subset \left\{ x \in \partial\Omega,\ \ \frac{\partial u_\Omega}{\partial n} = 0 \right\}$ may be strict.

In this context, we denote by $\Sigma_D = \overline{\Gamma_D} \cap \overline{\Gamma} \subset \partial\Omega$ (resp. $\Sigma_N = \overline{\Gamma_N} \cap \overline{\Gamma} \subset \partial\Omega$) the boundary between the region $\Gamma_D \subset \partial\Omega$ bearing homogeneous Dirichlet boundary conditions (resp. the region $\Gamma_N \subset \partial\Omega$ bearing inhomogeneous Neumann boundary conditions) and that Γ endowed with homogeneous Neumann boundary conditions; for simplicity, we assume that $\overline{\Gamma_D} \cap \overline{\Gamma_N} = \emptyset$. The sets Σ_D and Σ_N are both assumed to be smooth, codimension 1 submanifolds of $\partial\Omega$: in particular, they amount to collections of isolated points in the case $d = 2$, and to sets of smooth closed curves drawn on $\partial\Omega$ if $d = 3$. We denote by $n_{\Sigma_D} : \Sigma_D \to \mathbb{R}^d$ (resp. $n_{\Sigma_N} : \Sigma_N \to \mathbb{R}^d$) the unit normal vector to Σ_D (resp. Σ_N) pointing outward Γ_D (resp. Γ_N), inside the tangent plane to $\partial\Omega$; see Fig. 1 (left) for an illustration of these definitions.

On several occurrences, the rigorous mathematical analysis of this model will be greatly simplified under further simplifying assumptions; in particular, in some duly specified situations, we shall proceed under the following hypotheses, in the situation where $d = 2$:

$$\begin{gathered} \text{The region } \overline{\Gamma_D} \cap \overline{\Gamma} \text{ consists of only two points } \overline{\Gamma_D} \cap \overline{\Gamma} = \{s_0, s_1\}, \\ \text{and} \\ \text{the domain } \Omega \subset \mathbb{R}^2 \text{ is locally flat around } s_0, s_1; \end{gathered} \tag{2.3}$$

see Fig. 1 (right). In this last case, letting $n = (n_1, n_2)$, we shall denote by $\tau := (n_2, -n_1)$ the unit tangent vector to $\partial\Omega$, oriented so that (τ, n) is a direct orthonormal frame of the plane.

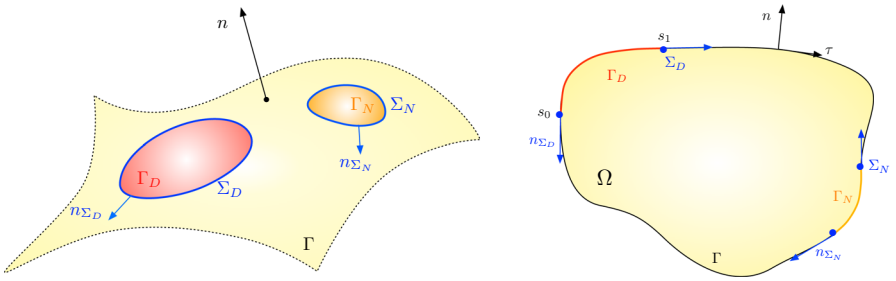

Fig. 1 (Left) Sketch of the considered setting in Sect. 2.1; (right) the simplified situation where Assumption (2.3) is fulfilled.

2.2 The shape optimization problem

In the setting of Sect. 2.1, we consider the following shape optimization problem:

$$\inf_{\Omega \in \mathcal{U}_{\text{ad}}} J(\Omega), \tag{2.4}$$

featuring an objective criterion $J(\Omega)$ of the form

$$J(\Omega) = \int_{\Omega} j(u_\Omega)\, dx \tag{2.5}$$

where $j : \mathbb{R} \to \mathbb{R}$ is a smooth function satisfying appropriate growth conditions: there exists a constant $C > 0$ such that:

$$\forall t \in \mathbb{R}, \quad |j(t)| \leq C(1 + t^2), \quad |j'(t)| \leq C(1 + |t|), \text{ and } |j''(t)| \leq C.$$

In (2.4), $\mathcal{U}_{\text{ad}}$ is a set of smooth admissible shapes; in the following, two distinct shape optimization problems of this form are considered, implying different definitions of $\mathcal{U}_{\text{ad}}$:

– On the one hand, the transition Σ_D between homogeneous Dirichlet and homogeneous Neumann boundary conditions is subject to optimization, and the region Γ_N bearing inhomogeneous Neumann boundary conditions is fixed. Then, $\mathcal{U}_{\text{ad}}$ corresponds to the set:

$$\mathcal{U}_{\mathrm{DN}} := \left\{ \Omega \subset \mathbb{R}^d \text{ is bounded and of class } \mathcal{C}^2, \quad \Gamma_N \subset \partial\Omega \right\}.$$

– On the other hand, when the region Σ_N between Γ and Γ_N is optimized (while the region $\Gamma_D \subset \partial\Omega$ is fixed), $\mathcal{U}_{\mathrm{ad}}$ reads:

$$\mathcal{U}_{\mathrm{NN}} := \left\{ \Omega \subset \mathbb{R}^d \text{ is bounded and of class } \mathcal{C}^2, \quad \Gamma_D \subset \partial\Omega \right\}.$$

Notice that problem (2.4) is not guaranteed to have a solution; nevertheless, we assume in the following that it is the case or that, at least, local minima exist. Moreover, observe that the objective function $J(\Omega)$ featured in (2.5) and the solution u_Ω to (2.2) depend on the particular subdivision (2.1) of the boundary $\partial\Omega$ into Γ_D, Γ_N and Γ; with some little abuse and so as to keep notations simple insofar as possible, this dependence is not made explicit in the formulation of our shape optimization problem.

Most practical optimization algorithms for solving problems of the form (2.4) rely on the derivative of $J(\Omega)$, which calls for a notion of differentiation with respect to the domain. Several ways are available to achieve this, and in the present work, we rely on Hadamard's boundary variation method; see e.g. [6,33,46,53]. In a nutshell, variations of a domain Ω are considered under the form:

$$\Omega_\theta := (\mathrm{Id} + \theta)(\Omega), \quad \theta \in W^{1,\infty}(\mathbb{R}^d, \mathbb{R}^d), \quad ||\theta||_{W^{1,\infty}(\mathbb{R}^d,\mathbb{R}^d)} < 1.$$

Accordingly, a function of the domain $F(\Omega)$ is said to be shape differentiable at Ω if the underlying mapping $\theta \mapsto F(\Omega_\theta)$, from $W^{1,\infty}(\mathbb{R}^d, \mathbb{R}^d)$ into $\mathbb{R}$, is Fréchet differentiable at $\theta = 0$. The following expansion then holds in the neighborhood of $\theta = 0$:

$$F(\Omega_\theta) = F(\Omega) + F'(\Omega)(\theta) + o(\theta), \text{ where } \frac{o(\theta)}{||\theta||_{W^{1,\infty}(\mathbb{R}^d,\mathbb{R}^d)}} \xrightarrow{\theta \to 0} 0. \quad (2.6)$$

In practice, so that variations of an admissible shape stay admissible, the considered deformations θ are confined to a subset $\Theta_{\mathrm{ad}} \subset W^{1,\infty}(\mathbb{R}^d, \mathbb{R}^d)$ of *admissible deformations*. In the present article, Θ_{ad} stands for one of the sets Θ_{DN} or Θ_{NN} defined by:

$$\Theta_{\mathrm{DN}} := \left\{ \theta \in \mathcal{C}^2(\mathbb{R}^d, \mathbb{R}^d) \cap W^{1,\infty}(\mathbb{R}^d, \mathbb{R}^d), \quad \theta = 0 \text{ on } \Gamma_N \right\}, \quad (2.7)$$

and

$$\Theta_{\mathrm{NN}} := \left\{ \theta \in \mathcal{C}^2(\mathbb{R}^d, \mathbb{R}^d) \cap W^{1,\infty}(\mathbb{R}^d, \mathbb{R}^d), \quad \theta = 0 \text{ on } \Gamma_D \right\}, \quad (2.8)$$

both being equipped with the natural norm, when the considered set of admissible shapes is $\mathcal{U}_{\mathrm{DN}}$ or $\mathcal{U}_{\mathrm{NN}}$, respectively.

Remark 1 In practice, it often turns out that the expression of the shape derivative $J'(\Omega)(\theta)$ of the considered objective function does not readily allow to identify a descent direction for $J(\Omega)$, that is, a deformation $\theta \in \Theta_{\text{ad}}$ such that $J'(\Omega)(\theta) < 0$. To remedy this difficulty, we rely on the 'change of inner products' strategy presented, e.g. in [14,21]: in a nutshell, a suitable Hilbert space $\mathcal{H} \subset \Theta_{\text{ad}}$ is selected, with inner product $a(\cdot, \cdot)$, and the gradient associated to the derivative $J'(\Omega)(\theta)$ via this inner product is calculated as the solution to the following problem:

$$\text{Search for } V \in \mathcal{H} \text{ s.t. } \forall \xi \in \mathcal{H}, \quad a(V, \xi) = J'(\Omega)(\xi). \tag{2.9}$$

It then follows immediately from (2.6) that $\theta = -V$ is a descent direction for $J(\Omega)$. A popular strategy consists in taking $\mathcal{H} = H^1(D)^d$ (where D is a large computational domain), equipped with the inner product

$$a(\theta, \xi) = \alpha^2 \int_D \nabla\theta : \nabla\xi \, dx + \int_D \theta \cdot \xi \, dx,$$

where the parameter α is chosen of the order of the mesh size; the resolution of (2.9) then boils down to that of a Laplace-like equation. Note that this choice is only formal (since $\mathcal{H}$ may not be contained in Θ_{ad}) but it turns out to work well in practice.

Remark 2 In principle, the shape optimization problem (2.4) could be supplemented with p constraints of the form

$$C_i(\Omega) \leq 0, \quad i = 1, \dots, p;$$

since this does not add anything to the points we intend to highlight in this article, but only increases the difficulty of the numerical treatment of (2.4), we ignore these issues.

2.3 A brief account of the regularity of u_Ω

As is well-known in the field of elliptic boundary value problems (see e.g. [2], or [13] §9.6 for a comprehensive introduction), when the featured data f, g (and Ω itself) are smooth enough, the solution u_Ω to (2.2) is more regular than a mere element in $H^1(\Omega)$, as predicted by the classical Lax-Milgram variational theory. For instance, in the 'simple' case where (2.2) only brings into play homogeneous Dirichlet boundary conditions (i.e. Γ and Γ_N are empty), the classical 'shift theorem' states that, provided f belongs to $H^m(\Omega)$ for some $m \geq 0$ (and Ω is smooth), u_Ω belongs to $H^{m+2}(\Omega)$.

In the situations at stake in the present article, such as (2.2), things are a little more subtle. The assumptions that $f \in L^2(\mathbb{R}^d)$ and $g \in H^1(\mathbb{R}^d)$ still guarantee that u_Ω has H^2 regularity in some open neighborhood of an arbitrary point x_0 which is either interior to Ω, or which belongs to $\partial\Omega$ but is interior to one of the regions Γ_D, Γ or Γ_N. On the contrary, u_Ω has limited regularity around those points $x_0 \in \Sigma_D$ or $x_0 \in \Sigma_N$ marking the transition between regions subjected to different types of boundary conditions. A whole mathematical theory exists in the literature, which is

devoted to the precise study of the 'weakly singular' behavior of u_Ω in these regions; we refer for instance to the monographs [20,30,37].

In this section, we first recall briefly some classical material about functional spaces in Sect. 2.3.1, before summarizing in Sect. 2.3.2 the needed results about the regularity of the solution u_Ω to (2.2) for our purposes.

2.3.1 Some functional spaces

Let Ω be a smooth bounded domain in $\mathbb{R}^d$. For $s > 0$ and $1 < p < \infty$, let us introduce:

– The usual Sobolev space $W^{s,p}(\Omega)$ is defined by, when $s = m$ is an integer:

$$W^{m,p}(\Omega) = \left\{ u \in L^p(\Omega),\ \ \partial^\alpha u \in L^p(\Omega) \text{ for } \alpha \in \mathbb{N}^d,\ \ |\alpha| \leq m \right\},$$

and when $s = m + \sigma$ with $m \in \mathbb{N}$ and $\sigma \in (0, 1)$,

$$W^{s,p}(\Omega) = \left\{ u \in W^{m,p}(\Omega),\ \ \int_\Omega \int_\Omega \frac{|\partial^\alpha u(x) - \partial^\alpha u(y)|^p}{|x - y|^{d+p\sigma}}\, dy\, dx < \infty \text{ for all } |\alpha| = m \right\}.$$

Both sets are equipped with the natural norms. Let us recall that the exact same definitions hold when the bounded domain Ω is replaced by the whole space $\mathbb{R}^d$.

– The subspace $\widetilde{W}^{s,p}(\Omega)$ of $W^{s,p}(\Omega)$ is that composed of functions whose extension $\widetilde{u}$ by 0 outside Ω belongs to $W^{s,p}(\mathbb{R}^d)$.

– The space $W_0^{s,p}(\Omega)$ is the closure of the set $\mathcal{C}_c^\infty(\Omega)$ of $\mathcal{C}^\infty$ functions with compact support in Ω in $W^{s,p}(\Omega)$.

As is customary, in the case $p = 2$ we use the notations $H^s(\Omega)$, $\widetilde{H}^s(\Omega)$ and $H_0^s(\Omega)$ for $W^{s,p}(\Omega)$, $\widetilde{W}^{s,p}(\Omega)$ and $W_0^{s,p}(\Omega)$ respectively.

In spite of their tight relation, the two spaces $\widetilde{W}^{s,p}(\Omega)$ and $W_0^{s,p}(\Omega)$ may not coincide depending on the values of s and p. On the one hand, for any $s > 0$ and $1 < p < \infty$, $W_0^{s,p}(\Omega) \subset \widetilde{W}^{s,p}(\Omega)$, but the converse inclusion may fail. In fact, the following characterization holds (see [30], Lemma 1.3.2.6 and Corollary 1.4.4.10):

$$\widetilde{W}^{s,p}(\Omega) = \left\{ u \in W_0^{m,p}(\Omega),\ \ \frac{1}{\rho^\sigma} \partial^\alpha u \in L^p(\Omega),\ \ |\alpha| = m \right\}, \tag{2.10}$$

where we have decomposed $s = m + \sigma$, with $m \in \mathbb{N}$ and $\sigma \in (0, 1)$, and $\rho(x) := d(x, \partial\Omega)$ is the (unsigned) distance from x to the boundary of Ω. The space $\widetilde{W}^{s,p}(\Omega)$ is then endowed with the norm

$$||u||_{\widetilde{W}^{s,p}(\Omega)} = \left(||u||^p_{W^{m,p}(\Omega)} + \sum_{|\alpha|=m} \int_\Omega \frac{1}{\rho^{p\sigma}} |\partial^\alpha u|^p\, dx \right)^{\frac{1}{p}}, \tag{2.11}$$

which is equivalent to the natural norm $u \mapsto ||\widetilde{u}||_{W^{s,p}(\mathbb{R}^d)}$. Let us also note that:

$$\widetilde{W}^{s,p}(\Omega) = W_0^{s,p}(\Omega) \text{ when } \left(s - \frac{1}{p}\right) \text{ is not an integer.}$$

We eventually mention that the above definitions and results hold in the more general context where Ω is replaced by a smooth submanifold of $\mathbb{R}^d$, e.g. (a region of) the boundary of a bounded smooth domain of $\mathbb{R}^d$. For instance, in the setting of Sect. 2.1, we may consider the spaces $\widetilde{W}^{s,p}(\Gamma_D)$, $\widetilde{W}^{s,p}(\Gamma_N)$, etc.

2.3.2 Local structure of u_Ω near the transition Σ_D

The classical variational theory for (2.2) (based on the Lax-Milgram theorem) features a solution u_Ω which naturally belongs to $H^1(\Omega)$. Moreover, assuming that the boundary $\partial\Omega$ is at least of class $\mathcal{C}^2$, and that $f \in L^2(\mathbb{R}^d)$, $g \in H^1(\mathbb{R}^d)$, the 'classical' elliptic regularity theory ensures that u_Ω actually has H^2 regularity except perhaps near the transitions zones Σ_D and Σ_N; see [2], and [13], §9.6. On the contrary, u_Ω fails to enjoy H^2 regularity in the vicinity of Σ_D or Σ_N, where the boundary conditions it fulfills change types.

The precise behavior of u_Ω near Σ_D will be of utmost interest for our purpose; it is exemplified by the following theorem, which takes place under Assumption (2.3) (see [30], Chap. 4 and notably Th. 4.4.3.7):

Proposition 1 *For any point $x_0 \in \Omega$ or $x_0 \in \partial\Omega \setminus (\Sigma_D \cup \Sigma_N)$, there exists an open neighborhood W of x_0 in $\mathbb{R}^2$ such that u_Ω belongs to $H^2(\Omega \cap W)$. Furthermore, for either $i = 0$ or $i = 1$, there exists an open neighborhood V of s_i with the following property: introducing the polar coordinates (r, v) at s_i, assuming without loss of generality that $s_i = 0$, $\Omega \cap V = \{x \in V,\ s.t.\ x_2 > 0\}$, and $\Gamma_D \cap V = \{x \in V,\ s.t.\ x_2 = 0,\ x_1 < 0\}$, there exist a function $u_r^i \in H^2(V)$, and a constant $c^i \in \mathbb{R}$ such that:*

$$u_\Omega = u_r^i + c^i S^i \text{ on } V, \text{ where } S^i(r, v) = r^{\frac{1}{2}} \cos\left(\frac{v}{2}\right). \tag{2.12}$$

The function S^i is sometimes said to be *weakly singular*, in the sense that it belongs to $H^1(V)$, but not to $H^2(V)$. More precisely, invoking Theorem 1.4.5.3 in [30] to estimate the Sobolev regularity of functions of the form $r^\alpha \varphi(v)$, one proves that, for every $0 \leq s < \frac{3}{2}$, $u_\Omega \in H^s(V)$, with:

$$||u_\Omega||_{H^s(V)} \leq C_s ||f||_{L^2(\mathbb{R}^d)}. \tag{2.13}$$

In the language of Sect. 2.3.1, it follows in particular that $u_\Omega \in \widetilde{H}^{\frac{1}{2}}(\Gamma \cup \Gamma_N)$, while $\frac{\partial u_\Omega}{\partial n} \in (\widetilde{H}^{\frac{1}{2}}(\Gamma \cup \Gamma_N))^*$.

Remark 3 Higher-order versions of the expansion (2.12) are available. Actually, for any integer $m \geq 2$, if $f \in H^{m-2}(\mathbb{R}^d)$, the following decomposition holds in a neighborhood V of s_i (see [30], Th. 5.1.3.5):

$$u_\Omega = u^i_{r,m} + \sum_{k=1}^{m-1} c^i_k S^i_k, \text{ where } u^i_{r,m} \in H^m(V) \text{ and}$$
$$S^i_k(r, \nu) = r^{k-\frac{1}{2}} \cos\left(\left(k - \frac{1}{2}\right)\nu\right).$$

Remark 4 Still in the two-dimensional context, when the boundary $\partial\Omega$ is not flat in the vicinity of Σ_D, an expansion of the form (2.12) still holds: the weakly singular function S^i shows the same dependence $r^{\frac{1}{2}}$ with respect to r, but its dependence with respect to ν is no longer explicit. Nevertheless, there still holds that $u_\Omega \in H^s(V)$ with an estimate of the form (2.13), where V is an open neigborhood of Σ_D in Ω and $0 \leq s < \frac{3}{2}$ is arbitrary; see [30], Chap. 5 or [18].

3 Shape derivatives of the functional $J(\Omega)$

In this section, we rigorously calculate the shape derivative of the objective function (2.4); we start in Sect. 3.1 with the case where the transition region Σ_N is optimized and Σ_D is fixed (i.e. the sets of admissible shapes and admissible deformations are $\mathcal{U}_{\mathrm{NN}}$ and Θ_{NN} respectively), before turning in Sect. 3.2 to the more difficult case where Σ_D is optimized and Σ_N is not—i.e. $\mathcal{U}_{\mathrm{ad}} = \mathcal{U}_{\mathrm{DN}}$ and $\Theta_{\mathrm{ad}} = \Theta_{\mathrm{DN}}$—under the simplifying assumption (2.3).

3.1 Calculation of the shape derivative of $J(\Omega)$ when only the homogeneous Neumann–inhomogeneous Neumann transition is optimized

Our main result in this section is the following.

Proposition 2 *The functional $J(\Omega)$ defined by (2.5) is shape differentiable over the admissible set $\mathcal{U}_{NN}$; its shape derivative reads (volumetric form):*

$$\forall \theta \in \Theta_{NN},\ J'(\Omega)(\theta) = \int_{\partial\Omega} (j(u_\Omega) - f p_\Omega)\theta \cdot n\, ds - \int_\Omega j'(u_\Omega)\nabla u_\Omega \cdot \theta\, dx$$
$$+ \int_\Omega (div\theta\, I - \nabla\theta - \nabla\theta^T)\nabla u_\Omega \cdot \nabla p_\Omega\, dx + \int_\Omega f \nabla p_\Omega \cdot \theta\, dx$$
$$- \int_{\Gamma_N} ((div_{\partial\Omega}\theta)g + \nabla g \cdot \theta) p_\Omega\, ds, \tag{3.1}$$

where $\mathrm{div}_{\partial\Omega}$ stands for the tangential divergence on $\partial\Omega$ (see Appendix A), and the adjoint state p_Ω is the unique solution in $H^1_{\Gamma_D}(\Omega)$ to the system:

$$\left\{\begin{array}{ll} -\Delta p_\Omega = -j'(u_\Omega) \text{ in } \Omega, & \\ p_\Omega = 0 & \text{on } \Gamma_D, \\ \frac{\partial p_\Omega}{\partial n} = 0 & \text{on } \Gamma_N \cup \Gamma. \end{array}\right. \tag{3.2}$$

The above shape derivative has the alternative, surfacic form:

$$\begin{aligned} \forall \theta \in \Theta_{NN},\ \ J'(\Omega)(\theta) = &\int_{\Gamma\cup\Gamma_N} j(u_\Omega)\theta\cdot n\, ds + \int_{\Gamma\cup\Gamma_N} \nabla u_\Omega\cdot\nabla p_\Omega\,\theta\cdot n\, ds \\ &- \int_{\Gamma\cup\Gamma_N} f p_\Omega\theta\cdot n\, ds - \int_{\Gamma_N}\left(\frac{\partial g}{\partial n} + \kappa g\right) p_\Omega\theta\cdot n\, ds \\ &- \int_{\Sigma_N} g p_\Omega\theta\cdot n_{\Sigma_N}\, d\ell, \end{aligned} \tag{3.3}$$

where the mean curvature κ of $\partial\Omega$ is defined in (A.1).

Remark 5 One comment is in order about the precise meaning of (3.3), and notably that of the term

$$\int_{\Gamma\cup\Gamma_N} \nabla u_\Omega\cdot\nabla p_\Omega\,\theta\cdot n\, ds \tag{3.4}$$

featured in there. The function u_Ω belongs to the space

$$E(\Delta, L^2(\Omega)) := \left\{u\in H^1(\Omega),\ \ \Delta u\in L^2(\Omega)\right\}, \tag{3.5}$$

and as such, it has a normal trace $\frac{\partial u_\Omega}{\partial n}\in H^{-1/2}(\partial\Omega)$, which is defined by the Green's formula:

$$\forall w\in H^1(\Omega),\ \ \int_{\partial\Omega}\frac{\partial u_\Omega}{\partial n} w\, ds := \int_\Omega \Delta u_\Omega w\, dx + \int_\Omega \nabla u_\Omega\cdot\nabla w\, dx; \tag{3.6}$$

see [30], Th. 1.5.3.10 for more details about this point. Also, since $u_\Omega\in H^{1/2}(\partial\Omega)$, the tangential derivative $\frac{\partial u_\Omega}{\partial\tau}$ naturally belongs to the dual space $H^{-1/2}(\partial\Omega)$. On the other hand, the function p_Ω enjoys H^2 regularity on account of elliptic regularity (see Sect. 2.3), except perhaps near Σ_D where it has a weak singularity of the form (2.12). Since deformations $\theta\in\Theta_{\mathrm{NN}}$ are smooth and vanish identically on Γ_D, the product $(\nabla p_\Omega)\theta\cdot n$ has a trace in $H^{1/2}(\partial\Omega)$, and so the integral (3.4) is well-defined as a duality product.

Proof The proof is an application of fairly classical techniques in shape optimization, except perhaps on one point regarding the regularity of u_Ω and p_Ω. Since variations of this argument are used in the following, we present a sketch of it for the reader's convenience. The proof is decomposed into two steps.

Step 1: Proof of the shape differentiability of $J(\Omega)$ and derivation of (3.1).

This step amounts to the analysis of the differentiability of the mapping $\theta \mapsto J(\Omega_\theta)$ from $\Theta_{\rm NN}$ into $\mathbb{R}$, which features the solution u_{Ω_θ} to the version of (2.2) posed on Ω_θ. The main idea consists in recasting the latter problem as a boundary-value problem on Ω for the transported function $\overline{u_\theta} := u_{\Omega_\theta} \circ (\mathrm{Id} + \theta) \in H^1(\Omega)$; thence, the implicit function theorem allows to calculate the derivative of the mapping $\theta \mapsto \overline{u_\theta}$; see [33,46].

For $\theta \in \Theta_{\rm NN}$ with norm $||\theta||_{\Theta_{\rm NN}} < 1$, the function u_{Ω_θ} is the unique solution in $H^1_{\Gamma_D}(\Omega_\theta)$ to the following variational problem:

$$\forall v \in H^1_{\Gamma_D}(\Omega_\theta), \quad \int_{\Omega_\theta} \nabla u_{\Omega_\theta} \cdot \nabla v \, dx = \int_{\Omega_\theta} f v \, dx + \int_{(\Gamma_N)_\theta} g v \, ds.$$

Using test functions of the form $v \circ (\mathrm{Id} + \theta)^{-1}$, $v \in H^1_{\Gamma_D}(\Omega)$, a change of variables yields the following variational formulation for $\overline{u_\theta} \in H^1_{\Gamma_D}(\Omega)$:

$$\begin{aligned} \forall v \in H^1_{\Gamma_D}(\Omega), \quad \int_\Omega A(\theta) \nabla \overline{u_\theta} \cdot \nabla v \, dx = & \int_\Omega |\det(\mathrm{I} + \nabla\theta)| f \circ (\mathrm{Id} + \theta) v \, dx \\ & + \int_{\Gamma_N} |\mathrm{com}(\mathrm{I} + \nabla\theta) n| g \circ (\mathrm{Id} + \theta) v \, ds, \end{aligned}$$

where $A(\theta)$ is the $d \times d$ matrix $A(\theta) = |\det(\mathrm{I} + \nabla\theta)|(\mathrm{I} + \nabla\theta)^{-1}(\mathrm{I} + \nabla\theta)^{-T}$ and $\mathrm{com}(M)$ stands for the cofactor matrix of a $d \times d$ matrix M. Now introducing the mapping $\mathcal{F} : \Theta_{\rm ad} \times H^1_{\Gamma_D}(\Omega) \to (H^1_{\Gamma_D}(\Omega))^*$ defined by:

$$\begin{aligned} \forall v \in H^1_{\Gamma_D}(\Omega), \quad \mathcal{F}(\theta, u)(v) = & \int_\Omega A(\theta) \nabla u \cdot \nabla v \, dx \\ & - \int_\Omega |\det(\mathrm{I} + \nabla\theta)| f \circ (\mathrm{Id} + \theta) v \, dx \\ & - \int_{\Gamma_N} |\mathrm{com}(\mathrm{I} + \nabla\theta) n| g \circ (\mathrm{Id} + \theta) v \, ds, \end{aligned}$$

it follows that for 'small' $\theta \in \Theta_{\rm NN}$, $\overline{u}_\theta$ is the unique solution of the equation $\mathcal{F}(\theta, \overline{u}_\theta) = 0$. Then, the implicit function theorem (see e.g. [38], Chap. 1, Th. 5.9) together with classical calculations imply that the mapping $\theta \mapsto \overline{u_\theta}$ is Fréchet differentiable from a neighborhood of 0 in $\Theta_{\rm NN}$ into $H^1_{\Gamma_D}(\Omega)$, and that its derivative $\theta \mapsto u'_\Omega(\theta)$ at $\theta = 0$—the so-called 'Lagrangian derivative' of the mapping $\Omega \mapsto u_\Omega$—is the unique solution to the following variational problem:

$$\begin{aligned} & \forall v \in H^1_{\Gamma_D}(\Omega), \int_\Omega \nabla u'_\Omega(\theta) \cdot \nabla v \, dx \\ & = - \int_\Omega (\mathrm{div}\theta \mathrm{I} - \nabla\theta - \nabla\theta^T) \nabla u_\Omega \cdot \nabla v \, dx \end{aligned}$$

$$+\int_\Omega \mathrm{div}(f\theta)v\,dx + \int_{\Gamma_N}((\mathrm{div}_{\partial\Omega}\theta)g + \nabla g\cdot\theta)\,v\,ds. \tag{3.7}$$

On the other hand, performing the same change of variables in the definition of $J(\Omega)$ yields:

$$J(\Omega_\theta) = \int_\Omega |\det(\mathrm{I}+\nabla\theta)|\; j(\overline{u_\theta})\,dx,$$

and so the mapping $\theta \mapsto J(\Omega_\theta)$ from Θ_{NN} into $\mathbb{R}$ is Fréchet differentiable at $\theta = 0$ with derivative:

$$J'(\Omega)(\theta) = \int_\Omega (\mathrm{div}\theta\; j(u_\Omega) + j'(u_\Omega)u_\Omega^\circ(\theta))\,dx. \tag{3.8}$$

The material derivative $u_\Omega^\circ(\theta)$ can now be eliminated from (3.8) thanks to the introduction of the adjoint state p_Ω, solution to (3.2). Indeed, the variational formulation of p_Ω reads:

$$\forall v \in H^1_{\Gamma_D}(\Omega),\quad \int_\Omega \nabla p_\Omega\cdot\nabla v\,dx = -\int_\Omega j'(u_\Omega)v\,dx. \tag{3.9}$$

Hence, combining (3.8) with (3.9) yields:

$$\begin{aligned}
J'(\Omega)(\theta) &= \int_\Omega (\mathrm{div}\theta)\,j(u_\Omega)\,dx - \int_\Omega \nabla p_\Omega\cdot\nabla u_\Omega^\circ(\theta)\,dx,\\
&= \int_\Omega (\mathrm{div}\theta)\,j(u_\Omega)\,dx + \int_\Omega ((\mathrm{div}\theta)\mathrm{I} - \nabla\theta - \nabla\theta^T)\nabla u_\Omega\cdot\nabla p_\Omega\,dx\\
&\quad - \int_\Omega \mathrm{div}(f\theta)p_\Omega\,dx - \int_{\Gamma_N}((\mathrm{div}_{\partial\Omega}\theta)g + \nabla g\cdot\theta)\,p_\Omega\,ds,\\
&= \int_\Omega \mathrm{div}(j(u_\Omega)\theta)\,dx - \int_\Omega j'(u_\Omega)\nabla u_\Omega\cdot\theta\,dx\\
&\quad + \int_\Omega ((\mathrm{div}\theta)\mathrm{I} - \nabla\theta - \nabla\theta^T)\nabla u_\Omega\cdot\nabla p_\Omega\,dx\\
&\quad - \int_\Omega \mathrm{div}(f\theta p_\Omega)\,dx + \int_\Omega f\nabla p_\Omega\cdot\theta\,dx\\
&\quad - \int_{\Gamma_N}((\mathrm{div}_{\partial\Omega}\theta)g + \nabla g\cdot\theta)\,p_\Omega\,ds,
\end{aligned}$$

where we have used the variational formulation (3.7) for $u_\Omega^\circ(\theta)$ to pass from the first line to the second one. This results in the desired expression (3.13). Note that at this point, we have not used the fact that either u_Ω or p_Ω is more regular than $H^1(\Omega)$.
Step 2: Derivation of the surface expression (3.3).

This expression is classically achieved from (3.1) using integration by parts; doing so requires a more careful attention to the regularity of u_Ω and p_Ω.

Let us notice that the function u_Ω may not be much more regular than just H^1 in the neighborhood of the transition Σ_N. Actually, it belongs to the space $E(\Delta, L^2(\Omega))$, defined by (3.5). The key point is that p_Ω is locally H^2 in the neighborhood of Σ_N, on account of the material in Sect. 2.3 (note that $\frac{\partial p_\Omega}{\partial n} = 0$ on $\Gamma \cup \Gamma_N$). Relying on the following identity, which holds for smooth functions $v, w \in \mathcal{C}_c^\infty(\mathbb{R}^d)$,

$$\begin{aligned}
&\int_\Omega ((\mathrm{div}\theta)\mathrm{I} - \nabla\theta - \nabla\theta^T)\nabla v \cdot \nabla w \, dx \\
&= \int_{\Gamma\cup\Gamma_N} \left((\nabla v \cdot \nabla w)\, \theta \cdot n - \frac{\partial v}{\partial n} \nabla w \cdot \theta - \frac{\partial w}{\partial n} \nabla v \cdot \theta \right) ds \\
&\quad + \int_\Omega (-\nabla(\nabla v \cdot \nabla w) + \Delta v \nabla w + \Delta w \nabla v \\
&\quad + \nabla^2 w \nabla v + \nabla^2 v \nabla w) \cdot \theta \, dx, \\
&= \int_{\Gamma\cup\Gamma_N} \left((\nabla v \cdot \nabla w)\, \theta \cdot n - \frac{\partial v}{\partial n} \nabla w \cdot \theta - \frac{\partial w}{\partial n} \nabla v \cdot \theta \right) ds \\
&\quad + \int_\Omega (\Delta v \nabla w + \Delta w \nabla v) \cdot \theta \, dx,
\end{aligned} \tag{3.10}$$

and using the density of $\mathcal{C}_c^\infty(\mathbb{R}^d)$ in $E(\Delta, L^2(\Omega))$ and $H^2(\Omega)$ (see [30], Lemma 1.5.3.9), we obtain:

$$\begin{aligned}
&\int_\Omega ((\mathrm{div}\theta)\mathrm{I} - \nabla\theta - \nabla\theta^T)\nabla u_\Omega \cdot \nabla p_\Omega \, dx \\
&= \int_{\Gamma\cup\Gamma_N} \left((\nabla u_\Omega \cdot \nabla p_\Omega)\, \theta \cdot n - \frac{\partial u_\Omega}{\partial n} \nabla p_\Omega \cdot \theta - \frac{\partial p_\Omega}{\partial n} \nabla u_\Omega \cdot \theta \right) ds \\
&\quad + \int_\Omega (\Delta u_\Omega \nabla p_\Omega + \Delta p_\Omega \nabla u_\Omega) \cdot \theta \, dx.
\end{aligned} \tag{3.11}$$

Let us now work on the last integral in the right-hand side of (3.1); we obtain:

$$\begin{aligned}
(\mathrm{div}_{\partial\Omega}\theta) g + \nabla g \cdot \theta &= \mathrm{div}_{\partial\Omega}(g\theta) + \tfrac{\partial g}{\partial n} \theta \cdot n, \\
&= \mathrm{div}_{\partial\Omega}(g(\theta - (\theta \cdot n)n)) + \left(\tfrac{\partial g}{\partial n} + \kappa g \right) \theta \cdot n.
\end{aligned}$$

Hence, an integration by parts on the region Γ_N using Proposition 7 yields:

$$\begin{aligned}
\int_{\Gamma_N} ((\mathrm{div}_{\partial\Omega}\theta) g + \nabla g \cdot \theta)\, p_\Omega \, ds &= \int_{\Sigma_N} g p_\Omega \, \theta \cdot n_{\Sigma_N} d\ell \\
&\quad + \int_{\Gamma_N} \left(\frac{\partial g}{\partial n} + \kappa g \right) p_\Omega \theta \cdot n \, ds.
\end{aligned} \tag{3.12}$$

Combining (3.11) and (3.12) with the volumetric formula (3.1) and using the facts that $-\Delta u_\Omega = f$ and $-\Delta p_\Omega = -j'(u_\Omega)$ in Ω, we finally obtain the desired surface formula (3.3). □

Remark 6 This calculation extends readily to the linearized elasticity case, to deal with Neumann–Neumann transitions.

3.2 Calculation of the shape derivative of $J(\Omega)$ when only the Dirichlet-homogeneous Neumann transition is optimized

In this section, we investigate the shape differentiability of the functional $J(\Omega)$ defined in (2.5) in the particular case where the boundary Σ_D between the regions Γ_D and Γ of $\partial\Omega$ bearing homogeneous Dirichlet and homogeneous Neumann boundary conditions is also subject to optimization; in other terms, we suppose:

$$\mathcal{U}_{\text{ad}} = \mathcal{U}_{\text{DN}}, \text{ and } \Theta_{\text{ad}} = \Theta_{\text{DN}}.$$

The main difficulty of the present situation lies in the weakly singular behavior of the solution u_Ω to (2.2) near Σ_D. In particular, the use of the formal Céa's method (see [15] and [6] for a comprehensive presentation), which implicitly relies on the smoothness of u_Ω, gives rise to an erroneous shape derivative in the present context.

The conclusion of Proposition 3 was already observed in [8,28], but our proof is slightly different: we rely on a direct calculation based on integration by parts.

Proposition 3 *The functional $J(\Omega)$ is shape differentiable at any admissible shape $\Omega \in \mathcal{U}_{DN}$, and its shape derivative reads (volumetric form):*

$$\begin{aligned}\forall \theta \in \Theta_{DN},\quad J'(\Omega)(\theta) = &\int_{\partial\Omega} (j(u_\Omega) - f p_\Omega)\theta \cdot n \, ds - \int_\Omega j'(u_\Omega)\nabla u_\Omega \cdot \theta \, dx \\ &+ \int_\Omega ((div\theta)I - \nabla\theta - \nabla\theta^T)\nabla u_\Omega \cdot \nabla p_\Omega \, dx \\ &+ \int_\Omega f \nabla p_\Omega \cdot \theta \, dx, \end{aligned} \tag{3.13}$$

where the adjoint state p_Ω is the unique solution in $H^1_{\Gamma_D}(\Omega)$ to the system:

$$\left\{ \begin{array}{ll} -\Delta p_\Omega = -j'(u_\Omega) & \text{in } \Omega, \\ p_\Omega = 0 & \text{on } \Gamma_D, \\ \frac{\partial p_\Omega}{\partial n} = 0 & \text{on } \Gamma_N \cup \Gamma. \end{array} \right. \tag{3.14}$$

Moreover, under the assumption (2.3), let us write the local structure of u_Ω and p_Ω in an open neighborhood V^i of s_i, $i = 0, 1$ as follows:

$$u_\Omega = u_s^i + u_r^i \text{ and } p_\Omega = p_s^i + p_r^i; \tag{3.15}$$

in the above formula, $u_r^i, p_r^i \in H^2(V^i)$ and the weakly singular functions u_s^i and $p_s^i \in H^1(V^i)$ have the following expressions in local polar coordinates centered at s_i:

$$u_s^i(r, \nu) = c_u^i r^{\frac{1}{2}} \cos\left(\frac{\nu}{2}\right), \text{ and } p_s^i(r, \nu) = c_p^i r^{\frac{1}{2}} \cos\left(\frac{\nu}{2}\right), \text{ if } n_{\Sigma_D}(s_i) = e_1 \tag{3.16}$$

or

$$u_s^i(r,v) = c_u^i r^{\frac{1}{2}} \sin(\frac{v}{2}), \text{ and } p_s^i(r,v) = c_p^i r^{\frac{1}{2}} \sin(\frac{v}{2}), \text{ if } n_{\Sigma_D}(s_i) = -e_1, \quad (3.17)$$

where (e_1, e_2) is the canonical basis of the plane. Then (3.13) rewrites (surface integral form):

$$J'(\Omega)(\theta) = \int_{\Gamma_D \cup \Gamma} (j(u_\Omega) - f p_\Omega)\theta \cdot n \, ds - \int_{\Gamma_D} \frac{\partial p_\Omega}{\partial n} \frac{\partial u_\Omega}{\partial n} \theta \cdot n \, ds + \int_{\Gamma} \frac{\partial u_\Omega}{\partial \tau} \frac{\partial p_\Omega}{\partial \tau} \theta \cdot n \, ds + \frac{\pi}{4} \sum_{i=0,1} c_u^i c_p^i (\theta \cdot n_{\Sigma_D})(s_i). \quad (3.18)$$

Remark 7 In the surface formula (3.18), the integrals

$$-\int_{\Gamma_D} \frac{\partial p_\Omega}{\partial n} \frac{\partial u_\Omega}{\partial n} \theta \cdot n \, ds + \int_{\Gamma} \frac{\partial u_\Omega}{\partial \tau} \frac{\partial p_\Omega}{\partial \tau} \theta \cdot n \, ds$$

are not well-defined individually, since they may blow up around the points s_i, as is quite clear from the look of the structure (3.16) and (3.17) of the singular parts of u_Ω and p_Ω. However, these integrals turn out to have compensating singularities at s_i, so that their sum is well-defined as a Cauchy principal value; see the proof below.

Proof The calculation of the volumetric formula (3.13) unfolds almost as in the case of Proposition 2, and we focus on the derivation of the surface formula (3.18), assuming that (2.3) holds. Again, the main idea of the calculation is to perform integration by parts from (3.13), taking advantage of the smoothness of u_Ω and p_Ω far from the singularities at s_i, $i = 0, 1$, and of the local structure (3.15) of these functions in the vicinity of s_i.

Let $\theta \in \Theta_{\mathrm{DN}}$ be fixed; for small $\delta > 0$, let $B^i(\delta) := B(s_i, \delta)$ be the ball centered at s_i with radius δ, and let $\Omega_\delta := \Omega \setminus (B^0(\delta) \cup (B^1(\delta))$. Since u_Ω and p_Ω belong to $H^1(\Omega)$, it holds from (3.13):

$$J'(\Omega)(\theta) = \int_{\partial\Omega} (j(u_\Omega) - f p_\Omega)\theta \cdot n \, ds + \lim_{\delta \to 0} I_\delta,$$

where:

$$I_\delta := -\int_{\Omega_\delta} j'(u_\Omega) \nabla u_\Omega \cdot \theta \, dx + \int_{\Omega_\delta} (\mathrm{div}\theta \mathrm{I} - \nabla\theta - \nabla\theta^T) \nabla u_\Omega \cdot \nabla p_\Omega \, dx + \int_{\Omega_\delta} f \nabla p_\Omega \cdot \theta \, dx.$$

Using the smoothness of u_Ω and p_Ω on Ω_δ, the fact that θ vanishes on Γ_N, the definitions of u_Ω, p_Ω and an integration by parts on the second term in the above

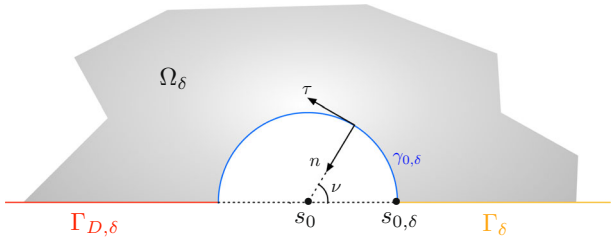

Fig. 2 The local situation around the point s_0 in the proof of Proposition 3

right-hand side based on the identity (3.10), we obtain:

$$I_\delta = \int_{\partial\Omega_\delta} \left(\nabla u_\Omega \cdot \nabla p_\Omega \, \theta \cdot n - \frac{\partial u_\Omega}{\partial n} \nabla p_\Omega \cdot \theta - \frac{\partial p_\Omega}{\partial n} \nabla u_\Omega \cdot \theta \right) ds. \quad (3.19)$$

To proceed further, we decompose the boundary $\partial\Omega_\delta$ as the disjoint reunion:

$$\partial\Omega_\delta = \Gamma_{D,\delta} \cup \Gamma_\delta \cup \Gamma_N \cup \gamma_{0,\delta} \cup \gamma_{1,\delta},$$

where $\Gamma_{D,\delta} = \Gamma_D \cap \Omega_\delta$, $\Gamma_\delta = \Gamma \cap \Omega_\delta$, and $\gamma_{i,\delta} = \partial B^i(\delta) \cap \Omega$ is the half-circle with center s_i and radius δ. We also denote by $s_{i,\delta}$ the intersection point between $\partial B^i(\delta)$ and Γ; see Fig. 2 about these notations.

Since $\theta = 0$ on Γ_N, it follows that:

$$\begin{aligned} I_\delta = & \int_{\Gamma_\delta} \frac{\partial u_\Omega}{\partial \tau} \frac{\partial p_\Omega}{\partial \tau} \theta \cdot n \, ds - \int_{\Gamma_{D,\delta}} \frac{\partial u_\Omega}{\partial n} \frac{\partial p_\Omega}{\partial n} \, \theta \cdot n \, ds \\ & + \sum_{i=0,1} \int_{\gamma_{i,\delta}} K(u_\Omega, p_\Omega) \, ds, \end{aligned} \quad (3.20)$$

where we have introduced the shorthand:

$$K(v, w) = \nabla v \cdot \nabla w \, \theta \cdot n - \frac{\partial v}{\partial n} \nabla w \cdot \theta - \frac{\partial w}{\partial n} \nabla v \cdot \theta.$$

Let us now evaluate the contributions of I_δ on $\gamma_{i,\delta}$ for $i = 0, 1$ in the expression (3.20). Without loss of generality, we only deal with $i = 0$, and we assume that $s_0 = 0$; according to (2.3), $\partial\Omega$ is horizontal in the neighborhood of s_0 and we also assume that Γ_D (resp. Γ) lies on the left-hand side (resp. the right-hand side) of s_0; see again Fig. 2. Introducing the polar coordinates (r, ν) with origin at $s_0 = 0$, taking into account our conventions for τ and n, we have:

$$n = -\cos\nu e_1 - \sin\nu e_2, \quad \tau = -\sin\nu e_1 + \cos\nu e_2,$$

and as far as derivatives are concerned:

$$\frac{\partial}{\partial n} = -\frac{\partial}{\partial r}, \text{ and } \frac{\partial}{\partial \tau} = \frac{1}{r} \frac{\partial}{\partial \nu}.$$

Recalling the local expressions (3.15) of u_Ω and p_Ω around s_0, it is easily seen that the only possibly non vanishing contribution of $\int_{\gamma_{0,\delta}} K(u_\Omega, p_\Omega)\, ds$ in the limit $\delta \to 0$ is given by the most singular part of its integrand:

$$\lim_{\delta\to 0}\int_{\gamma_{0,\delta}} K(u_\Omega, p_\Omega)\, ds = \lim_{\delta\to 0} \widetilde{I}^0_\delta, \text{ where } \widetilde{I}^0_\delta := \int_{\gamma_{0,\delta}} K(u^0_s, p^0_s)\, ds.$$

Let us then calculate the last integral. We have, on $\gamma_{0,\delta}$:

$$\begin{aligned}(\nabla u^0_s \cdot \nabla p^0_s)(\theta\cdot n) &= \left(\frac{\partial u^0_s}{\partial \tau}\frac{\partial p^0_s}{\partial \tau} + \frac{\partial u^0_s}{\partial n}\frac{\partial p^0_s}{\partial n}\right)(\theta\cdot n),\\ &= \left(\frac{1}{r^2}\frac{\partial u^0_s}{\partial \nu}\frac{\partial p^0_s}{\partial \nu} + \frac{\partial u^0_s}{\partial r}\frac{\partial p^0_s}{\partial r}\right)(\theta\cdot n),\\ &= \left(\frac{c^0_u c^0_p}{4r}\right)(\theta\cdot n).\end{aligned} \tag{3.21}$$

Likewise,

$$\begin{aligned}-\frac{\partial u^0_s}{\partial n}\nabla p^0_s\cdot\theta &= -\frac{\partial u^0_s}{\partial n}\frac{\partial p^0_s}{\partial \tau}\theta\cdot\tau - \frac{\partial u^0_s}{\partial n}\frac{\partial p^0_s}{\partial n}\theta\cdot n,\\ &= \frac{1}{r}\frac{\partial u^0_s}{\partial r}\frac{\partial p^0_s}{\partial \nu}\theta\cdot\tau - \frac{\partial u^0_s}{\partial r}\frac{\partial p^0_s}{\partial r}\theta\cdot n,\\ &= -\frac{c^0_u c^0_p}{4r}\cos\left(\frac{\nu}{2}\right)\sin\left(\frac{\nu}{2}\right)\theta\cdot\tau - \frac{c^0_u c^0_p}{4r}\cos^2(\tfrac{\nu}{2})\theta\cdot n,\end{aligned} \tag{3.22}$$

and

$$\begin{aligned}-\frac{\partial p^0_s}{\partial n}\nabla u^0_s\cdot\theta &= -\frac{\partial u^0_s}{\partial n}\nabla p^0_s\cdot\theta\\ &= -\frac{c^0_u c^0_p}{4r}\cos\left(\frac{\nu}{2}\right)\sin\left(\frac{\nu}{2}\right)\theta\cdot\tau - \frac{c^0_u c^0_p}{4r}\cos^2\left(\frac{\nu}{2}\right)\theta\cdot n.\end{aligned} \tag{3.23}$$

Gathering (3.21) to (3.23), we now obtain:

$$\begin{aligned}K(u^0_s, p^0_s) &= \frac{c^0_u c^0_p}{4r}\left((1-2\cos^2(\tfrac{\nu}{2}))\theta\cdot n - 2\cos\left(\frac{\nu}{2}\right)\sin\left(\frac{\nu}{2}\right)\theta\cdot\tau\right),\\ &= \frac{c^0_u c^0_p}{4r}\left(-(\sin\nu)\theta\cdot\tau - (\cos\nu)\theta\cdot n\right),\\ &= \frac{c^0_u c^0_p}{4r}\theta_1,\end{aligned}$$

where θ_1 is the horizontal component of $\theta = \theta_1 e_1 + \theta_2 e_2$. Therefore:

$$\widetilde{I}^0_\delta = \left(\int_0^\pi \frac{c^0_u c^0_p}{4}\theta_1(\delta\cos\nu, \delta\sin\nu)\, d\nu\right) \xrightarrow{\delta\to 0} \frac{\pi c^0_u c^0_p}{4}\theta_1(0).$$

Combining all these results, we obtain the surface form (3.18) of the shape derivative $J'(\Omega)(\theta)$. □

Remark 8 The result extends to the case where the boundary $\partial\Omega$ is not flat (but is still smooth) in the neighborhood of $\Sigma_D = \{s_0, s_1\}$. More precisely, let V be a small enough neighborhood of either of the s_i, and let us introduce a local description of Ω as a graph, assuming for simplicity that $s_i = 0$ and $n(s_i) = -e_2$: U is a neighborhood of 0 in $\mathbb{R}^2$ and $\psi(x_1, x_2) = (x_1, \varphi(_2))$ is a smooth diffeomorphism from U onto V such that:

$$\Omega \cap V = \left\{x = (x_1, x_2) \in \mathbb{R}^2, \;\; x_2 > \varphi(x_1)\right\} \cap U.$$

Then, it follows from [30], §5.2 that u_Ω reads in this case:

$$u_\Omega = c^i S^i \circ \psi^{-1} + u_r^i \text{ on } B_\delta(s_i),$$

where $u_r^i \in H^2(V)$. The proof extends to this latter context then.

Remark 9
- Interestingly, if u_Ω and p_Ω are assumed to be actually smooth (say H^2) in the neighborhood of the transition points s_0 and s_1, the shape derivative (3.18) no longer involves any term related to the geometry of the repartition of Γ_D and Γ. In other terms, all the information about the sensitivity of $J(\Omega)$ with respect to the repartition of Γ_D and Γ is encoded in the (weak) singularities of u_Ω and p_Ω.
- The fact that the sensitivity of $J(\Omega)$ with respect to variations of Σ_D in (3.18) involves the singular behavior of u_Ω and p_Ω near Σ_D is reminiscent of the field of fracture mechanics. There, the so-called Irwin formula relates the singularity of the elastic displacement of a material at the tip of a crack to the energy release rate guiding the growth of the crack; see [43].

4 An approximate shape optimization problem to deal with the Dirichlet–Neumann transition

We have calculated in Sect. 3 the shape derivative of the functional $J(\Omega)$ given by (2.5), in the situation where either the transition Σ_N or Σ_D is subject to optimization. The resulting expression in the former case (see Proposition 2) may be readily used in a typical gradient-based shape optimization algorithm; see Sect. 5.

On the other hand, in the case where Σ_D is optimized, the expression supplied by Proposition 3 is unfortunately awkward from both the theoretical and practical perspectives. Indeed,

- The calculation of the surface form (3.18) of $J'(\Omega)(\theta)$ was enabled by the precise knowledge of the local behavior (3.15) of u_Ω and p_Ω near the singularities s_0 and s_1. In more involved situations, for instance in three space dimensions, or in more challenging physical contexts (such as those of the linearized elasticity system, or the Stokes equations), such precise information may not be available, or may be difficult to handle.
- The numerical evaluation of the shape derivative $J'(\Omega)(\theta)$ requires the calculation of the coefficients c_u and c_p featured in (3.15); this is doable, but it demands adapted numerical techniques, for instance an enrichment of the finite element

basis with the singular functions, or adapted p/hp finite mesh refinement methods; see [9,27,39] and the references therein. In our numerical setting, presented in Sect. 5, such techniques are bound to be all the more difficult to carry out that the boundary Σ_D is not explicitly discretized in the computational mesh.
– Eventually, it is possible in principle to rely only on the volumetric form (3.13) of the shape derivative for algorithmic purposes, as is suggested for instance in [29,35] and the references therein; nevertheless, for many practical purposes, it is interesting to have a surface expression for this shape derivative—for instance when it comes to using advanced optimization algorithms such as that introduced in [26].

We thenceforth focus our efforts on the instance of the problem (2.4) where this transition zone Σ_D is also subject to optimization (while Σ_N is not). To overcome the aforementioned difficulties, we introduce an approximation method which allows for the optimization of the boundary Σ_D between regions bearing homogeneous Dirichlet and Neumann boundary conditions, without requiring the knowledge of the weakly singular behavior of u_Ω (and that of the adjoint state p_Ω) in the neighborhood of Σ_D. As we shall see in Sect. 5, this method lends itself to an easy generalization to more difficult situations: transitions between other types of boundary conditions involving a singular state, other physical contexts than that of the Laplace equation, etc.

Throughout this section, unless stated otherwise, we consider the shape optimization problem (2.4) in the physical setting of Sect. 2, in the particular case where the transition Σ_D between the regions Γ_D and Γ of $\partial\Omega$ is subject to optimization: $\mathcal{U}_{\mathrm{ad}} = \mathcal{U}_{\mathrm{DN}}$ and $\Theta_{\mathrm{ad}} = \Theta_{\mathrm{DN}}$. After introducing a few notations and background material regarding the notion of geodesic distance function in Sects. 4.1, 4.2, we present an approximate version of the physical problem (2.2), relying on a 'small' parameter $\varepsilon > 0$, with the noticeable feature that its unique solution $u_{\Omega,\varepsilon}$ is smooth. This leads to the introduction of an approximate shape optimization problem of a smoothed functional $J_\varepsilon(\Omega)$ in Sect. 4.3; we calculate the shape derivative $J'_\varepsilon(\Omega)(\theta)$ by classical means, and the numerical evaluation of the resulting expression poses no particular difficulty. Finally, in Sect. 4.4, we prove in the model context where (2.3) holds that the approximate shape optimization problem converges to its exact counterpart, in the sense that $u_{\Omega,\varepsilon} \to u_\Omega$ as $\varepsilon \to 0$, and the values of $J_\varepsilon(\Omega)$ and $J'_\varepsilon(\Omega)(\theta)$ converge to their exact counterparts $J(\Omega)$ and $J'(\Omega)(\theta)$.

4.1 About the signed distance function to a subset on a manifold

In this section, we collect some material about the signed distance function to a subregion of an oriented, closed and smooth submanifold $\mathcal{M}$ of $\mathbb{R}^d$ with codimension 1; $\mathcal{M}$ is equipped with a Riemannian structure by endowing its tangent bundle with the inner product induced by that of $\mathbb{R}^d$ and we denote by n its unit normal vector. In the context of Sect. 2, $\mathcal{M}$ stands for the boundary $\partial\Omega$ of the considered shape Ω.

Let us first set some notations and recall some necessary background material from Riemannian geometry; for these matters, we refer to [25].

The length $\ell(\gamma)$ of a piecewise differentiable curve $\gamma : I \to \mathcal{M}$ defined on an interval $I \subset \mathbb{R}$ is

$$\ell(\gamma) = \int_I |\gamma'(t)|\, dt.$$

The geodesic distance $d^{\mathcal{M}}(x, y)$ between two points $x, y \in \mathcal{M}$ is then:

$$d^{\mathcal{M}}(x, y) = \inf \ell(\gamma),$$

where the infimum is taken over all piecewise differentiable curves $\gamma : (a, b) \to \mathcal{M}$ such that $\gamma(a) = x$ and $\gamma(b) = y$. Likewise, we denote by

$$d^{\mathcal{M}}(x, K) = \inf_{y \in K} d^{\mathcal{M}}(x, y)$$

the distance between $x \in \mathcal{M}$ and a subset $K \subset \mathcal{M}$.

The notion of distance on $\mathcal{M}$ is conveniently described in terms of the *exponential mapping*: for any point $p \in \mathcal{M}$ and vector v in the tangent plane $T_p\mathcal{M}$ to $\mathcal{M}$ at p, $\exp_p(v)$ stands for the point $\gamma(1, p, v)$, where $t \mapsto \gamma(t, p, v)$ is the unique geodesic curve on $\mathcal{M}$ such that

$$\gamma(0) = p, \text{ and } \gamma'(0) = v.$$

As a well-known fact in Riemannian geometry, the mapping $\exp_p$ is well-defined on an open neighborhood U of 0 in $T_p\Gamma$ and it is a diffeomorphism from U onto an open neighborhood V of p in $\mathcal{M}$. The reciprocal mapping is the *logarithm* $\log_p : V \to U$:

$$\forall y \in V, \ \log_p(y) = \text{the unique } v \in U \text{ s.t. } \gamma(1, p, v) = y.$$

We now turn to the notion of signed distance function on the submanifold $\mathcal{M}$: let $G \subset \mathcal{M}$ be an open subset which we assume to be *smooth* for simplicity; its boundary $\Sigma := \partial G$ is a closed, smooth submanifold of $\mathbb{R}^d$ with codimension 2, and we denote by $n_\Sigma : \Sigma \to \mathbb{S}^1$ the unit normal vector to Σ pointing outward G. In particular, n_Σ is a vector field along Σ which is tangential to $\mathcal{M}$.

Definition 1 The signed distance function d_G to G is defined by:

$$\forall x \in \mathcal{M}, \ d_G(x) = \begin{cases} -d^{\mathcal{M}}(x, \Sigma) & \text{if } x \in G, \\ 0 & \text{if } x \in \Sigma, \\ d^{\mathcal{M}}(x, \Sigma) & \text{if } x \in \mathcal{M} \setminus \overline{G}. \end{cases}$$

For $y \in \mathcal{M}$, we denote by $p_\Sigma(y)$ the *projection* of y onto Σ, that is, the unique point $x \in \Sigma$ such that $d^{\mathcal{M}}(x, y) = d^{\mathcal{M}}(x, \Sigma)$, when this makes sense (i.e. when there is indeed such a unique point).

The following theorem states in essence that, when G is a regular subset of $\mathcal{M}$, the projection mapping p_Σ is well-defined and smooth on a neighborhood of Σ. The

proof is essentially the same as that of Theorem 3.1 in [7]: it is a local argument relying on the implicit function theorem, and we omit the details for brevity.

Theorem 1 *Let G be a regular open subset of $\mathcal{M}$; then there exists an open neighborhood $U \subset \mathcal{M}$ of Σ such that the mapping*

$$\Sigma \times (-t_0, t_0) \to U, \quad \mathcal{F}(x,t) = exp_x(t n_\Sigma(x))$$

is a diffeomorphism of class $\mathcal{C}^\infty$. For $y = \mathcal{F}(x,t) \in U$, one has:

$$t = d_G(y), \text{ and } x = p_\Sigma(y).$$

Let us now state a result about the (tangential) gradient of the distance function; the proof of the first point lies e.g. in [54], while the second one follows from a direct application of the theorem of differentiation of a minimum value (see [23], Chap. 10, Th. 2.1):

Proposition 4 – *Let $p \in \mathcal{M}$; consider the function $\rho(x) := d^{\mathcal{M}}(x, p)$ on a neighborhood U of p. Then ρ is differentiable on $U \setminus \{p\}$ and its (tangential) gradient reads:*

$$\nabla\rho(x) = -\frac{1}{d^{\mathcal{M}}(x,p)} log_x(p).$$

– *Let G be a regular open subset of $\mathcal{M}$ with boundary Σ, and let U be the neighborhood supplied by Theorem 1. Then the signed distance function d_G is differentiable at any point $x \in U$, and its gradient reads:*

$$\nabla d_G(x) = -\frac{1}{d_G(x)} log_x(p_\Sigma(x)).$$

We eventually consider the differentiation of the signed distance function d_G with respect to variations of the manifold $\mathcal{M}$ (and thus of Σ). The following result is new to the best of our knowledge:

Proposition 5 *Let G be a regular open subset of $\mathcal{M}$, and let U be the neighborhood of $\Sigma = \partial G$ supplied by Theorem 1. consider a fixed point $y \in U \setminus \Sigma$, and let $p = p_\Sigma(y)$, so that $\sigma(t) = exp_p(t n_\Sigma(p))$ is the unique geodesic joining p to y, parametrized by arc length. For any vector field $\theta \in \mathcal{C}^{1,\infty}(\mathbb{R}^d, \mathbb{R}^d)$, we define the variations of $\mathcal{M}$ and G according to Hadamard's method (see Sect. 2.2):*

$$\mathcal{M}_\theta = (Id + \theta)(\mathcal{M}), \text{ and } G_\theta = (Id + \theta)(G).$$

Define:

$$D(\theta) = d_{G_\theta}(y + \theta(y)).$$

Then D is Fréchet differentiable at $\theta = 0$ and its derivative reads:

$$D'(0)(\theta) = -\theta(y) \cdot \frac{\log_y(p)}{d_G(y)} - \theta(p) \cdot n_\Sigma(p) + \int_0^{d_G(y)} \Pi^{\mathcal{M}}_{\sigma(t)}(\sigma'(t), \sigma'(t))\, (\theta \cdot n)(\sigma(t))\, dt. \tag{4.1}$$

In the above formula, $\Pi^{\mathcal{M}}_p$ is the second fundamental form of $\mathcal{M}$ at p, that is:

$$\forall v \in T_p\mathcal{M}, \quad \Pi^{\mathcal{M}}_p v \cdot v = -\nabla n(p) v \cdot v,$$

where n is any extension of the normal vector $n : \mathcal{M} \to \mathbb{R}^d$ to an open neighborhood of $\mathcal{M}$ in $\mathbb{R}^d$.

Proof Assume for simplicity that $y \in \mathcal{M} \setminus \overline{G}$, the result being proved in a similar same way if $y \in G$. From the definition of $D(\theta)$, one has:

$$\begin{aligned} D(\theta) &= \inf_{x \in \Sigma} \inf_{\substack{\gamma:(a,b)\to\mathcal{M}_\theta \\ \gamma(a)=x+\theta(x),\ \gamma(b)=y+\theta(y)}} \int_a^b |\gamma'(t)|\, dt, \\ &= \inf_{x \in \Sigma} \inf_{\substack{\gamma:(a,b)\to\mathcal{M} \\ \gamma(a)=x,\ \gamma(b)=y}} \int_a^b \sqrt{(\mathrm{I} + \nabla\theta^T(\gamma(t)))(I + \nabla\theta(\gamma(t)))\gamma'(t) \cdot \gamma'(t)}\, dt, \end{aligned}$$

and we know that, for $\theta = 0$, this infimum is attained uniquely for $x = p$ and $\gamma = \sigma$, the geodesic curve joining p to y. Therefore, the theorem of differentiation through a minimum (see again [23], Chap. 10, Th. 2.1) entails that D is differentiable at $\theta = 0$ and:

$$D'(0)(\theta) = \int_a^b \frac{1}{|\sigma'(t)|} \nabla\theta(\sigma(t))\sigma'(t) \cdot \sigma'(t)\, dt.$$

Since $\sigma(t) = \exp_p(t n_\Sigma(p))$ is parametrized by arc length, we have in particular $|\sigma'(t)| = 1$, $\sigma(0) = p$ and $\sigma(d_G(y)) = y$ (that is, $a = 0$ and $b = d_G(y)$ in the above formula); therefore,

$$D'(0)(\theta) = \int_0^{d_G(y)} \nabla\theta(\sigma(t))\sigma'(t) \cdot \sigma'(t)\, dt = \int_0^{d_G(y)} (\theta(\sigma(t)))' \cdot \sigma'(t)\, dt,$$

whence, using integration by parts:

$$D'(0)(\theta) = \theta(y) \cdot \sigma'(d_G(y)) - \theta(p) \cdot \sigma'(0) - \int_0^{d_G(y)} \theta(\sigma(t)) \cdot \sigma''(t)\, dt.$$

In the above formula, it follows from the definition of σ and Proposition 4 that:

$$\sigma'(0) = n_\Sigma(p), \text{ and } \sigma'(d_G(y)) = -\frac{\log_y(p)}{d_G(y)}.$$

On the other hand, it follows from the fact that σ is a geodesic that:

$$\sigma''(t) \cdot v = 0 \text{ for any tangent vector } v \in T_{\sigma(t)}\mathcal{M};$$

see [25], Chap. 2, Exercise 4. Since in addition $\sigma'(t) \cdot n(\sigma(t)) = 0$, differentiation with respect to t yields:

$$\sigma''(t) \cdot n(\sigma(t)) = -\nabla n(\sigma(t))\sigma'(t) \cdot \sigma'(t) = \Pi^{\mathcal{M}}_{\sigma(t)}(\sigma'(t), \sigma'(t)),$$

which terminates the proof. □

Remark 10 – The formula (4.1) is of 'Lagrangian' nature: for given $y \in \mathcal{M}$, the derivative of the distance function to the perturbed set G_θ at the perturbed point $y + \theta(y)$ is calculated. Using the more classical notation $\mathring{d}_G(\theta)(y) = D'(0)(\theta)$ for this derivative, the corresponding *Eulerian* derivative $d'_G(\theta)(y)$ of d_G at y is then defined by the formula:

$$\begin{aligned} d'_G(\theta)(y) &:= \mathring{d}_G(\theta)(y) - \nabla d_G(y) \cdot \theta, \\ &= -\theta(p) \cdot n_\Sigma(p) + \int_0^{d_G(y)} \Pi^{\mathcal{M}}_{\sigma(t)}(\sigma'(t), \sigma'(t))\ (\theta \cdot n)(\sigma(t))\, dt, \end{aligned}$$

where we have used Proposition 4.

– The structure of (4.1) is quite intuitive: the first two terms are exactly those featured in the formula for the 'Lagrangian' derivative of the signed distance function in the Euclidean case, i.e. without taking into account the curvature of the ambient space (see e.g. [19]), while the last one expresses the deformation with respect to θ of the geodesic between p and y out of the (normal) variation of the manifold $\mathcal{M}$.

4.2 The smoothed setting

In the setting of Sect. 2 (see also Fig. 1), and following the works [4,24], we trade the solution u_Ω to the 'exact' problem (2.2) for that $u_{\Omega,\varepsilon}$ to the following approximate version, where the homogeneous Dirichlet and Neumann boundary conditions on Γ_D and Γ respectively are replaced by a Robin boundary condition on $\Gamma_D \cup \Gamma$:

$$\begin{cases} -\Delta u_{\Omega,\varepsilon} = f & \text{in } \Omega, \\ \frac{\partial u_{\Omega,\varepsilon}}{\partial n} + h_\varepsilon u_{\Omega,\varepsilon} = 0 & \text{on } \Gamma \cup \Gamma_D, \\ \frac{\partial u_{\Omega,\varepsilon}}{\partial n} = g & \text{on } \Gamma_N. \end{cases} \tag{4.2}$$

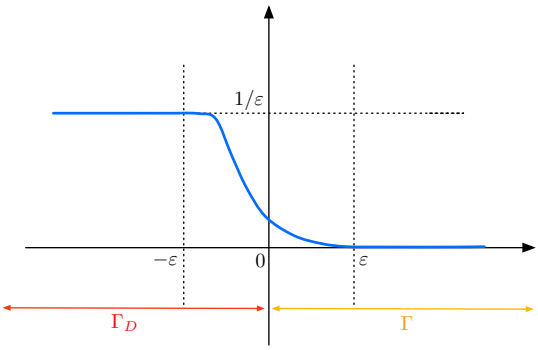

Fig. 3 Graph of the function h_ε defined by (4.3)

Here, the coefficient h_ε is defined by:

$$h_\varepsilon(x) = \frac{1}{\varepsilon} h\left(\frac{d_{\Gamma_D}(x)}{\varepsilon}\right), \tag{4.3}$$

where $h : \mathbb{R} \to \mathbb{R}$ is a smooth function with the properties:

$$0 \leq h \leq 1, \quad h \equiv 1 \text{ on } (-\infty, -1], \quad h(0) > 0, \quad h \equiv 0 \text{ on } [1, \infty),$$

and $d_{\Gamma_D}(x)$ is the (geodesic) signed distance function to Γ_D on the surface $\partial\Omega$; see Definition 1. In other words, h_ε equals $\frac{1}{\varepsilon}$ inside Γ_D, 'far' from Σ_D, 0 on Γ 'far' from Σ_D, and it presents a smooth transition between these two values in a tubular neighborhood of Σ_D with (geodesic) width ε, so that the boundary conditions in (2.2) are approximately satisfied; see Fig. 3.

In particular, h_ε vanishes on a neighborhood of Γ_N in $\partial\Omega$; notice also that our assumptions on h imply that there exists a real value $\alpha > 0$ which is independent of ε such that:

$$\forall x \in \Gamma_D, \quad \alpha \leq \varepsilon h_\varepsilon(x). \tag{4.4}$$

The variational formulation associated to (4.2) reads: $u_{\Omega,\varepsilon}$ is the unique function in $H^1(\Omega)$ such that

$$\begin{aligned} \forall v \in H^1(\Omega), \quad & \int_\Omega \nabla u_{\Omega,\varepsilon} \cdot \nabla v \, dx + \int_{\Gamma_D \cup \Gamma} h_\varepsilon u_{\Omega,\varepsilon} v \, ds \\ & = \int_\Omega f v \, dx + \int_{\Gamma_N} g v \, ds. \end{aligned} \tag{4.5}$$

It follows from the standard Lax-Milgram theory that this problem is well-posed. In addition, for a fixed value of $\varepsilon > 0$, due to the smoothness of Ω and h_ε (see Sect. 4.1 about the smoothness of d_{Γ_D}), the solution $u_{\Omega,\varepsilon}$ to (4.2) actually enjoys H^2 regularity on a neighborhood of Σ_D, as a consequence of the standard regularity theory for elliptic equations; see e.g. [13], Chap. 9.

Remark 11 This approximation method can be straightforwardly adapted to different contexts, such as that of the linearized elasticity system; see Sect. 5 for illustrations, and [24] for an adaptation in the context of the acoustic Helmholtz equation.

Remark 12 Admittedly, the choice (4.3) for the coefficient h_ε in the Robin boundary condition of (4.2) on $\Gamma_D \cup \Gamma$ approximating homogeneous Dirichlet boundary conditions on Γ_D and homogeneous Neumann boundary conditions on Γ is not unique. Roughly speaking, "any" function showing a smooth and fast transition between "very large" values on Γ_D, and "very small" values on Γ, with the condition (4.4) satisfied would lead to conclusions similar to those in the next sections.

4.3 The approximate shape optimization problem

We propose to replace the exact shape optimization problem (2.4) by its regularized counterpart:

$$\inf_{\Omega \in \mathcal{U}_{\mathrm{DN}}} J_\varepsilon(\Omega), \text{ where } J_\varepsilon(\Omega) := \int_\Omega j(u_{\Omega,\varepsilon})\, dx, \tag{4.6}$$

and $u_{\Omega,\varepsilon}$ is the solution to (4.2).

When it comes to the shape derivative of $J_\varepsilon(\Omega)$, the result of interest is the following:

Proposition 6 *The functional $J_\varepsilon(\Omega)$ is shape differentiable at any admissible shape $\Omega \in \mathcal{U}_{DN}$, and its shape derivative reads, for arbitrary $\theta \in \Theta_{DN}$ (volumetric form):*

$$\begin{aligned}
J'_\varepsilon(\Omega)(\theta) = &\int_{\partial\Omega} (j(u_{\Omega,\varepsilon}) - f p_{\Omega,\varepsilon})\, \theta \cdot n\, ds - \int_\Omega j'(u_{\Omega,\varepsilon}) \nabla u_{\Omega,\varepsilon} \cdot \theta\, dx \\
&+ \int_\Omega (div\theta I - \nabla\theta - \nabla\theta^T) \nabla u_{\Omega,\varepsilon} \cdot \nabla p_{\Omega,\varepsilon}\, dx \\
&+ \int_{\Gamma\cup\Gamma_D} (div_{\partial\Omega})\theta\, h_\varepsilon u_{\Omega,\varepsilon} p_{\Omega,\varepsilon}\, ds + \int_\Omega f \nabla p_{\Omega,\varepsilon} \cdot \theta\, dx \\
&+ \frac{1}{\varepsilon^2} \int_{\Gamma\cup\Gamma_D} h'\Big(\frac{d_{\Gamma_D}}{\varepsilon}\Big) \Bigg(-\theta(x) \cdot \frac{\log_x(p_{\Sigma_D}(x))}{d_{\Gamma_D}(x)} \\
&- \theta(p_{\Sigma_D}(x)) \cdot n_{\Sigma_D}(p_{\Sigma_D}(x)) \Bigg) u_{\Omega,\varepsilon} p_{\Omega,\varepsilon}\, ds(x) \\
&\frac{1}{\varepsilon^2} \int_{\Gamma\cup\Gamma_D} h'\Big(\frac{d_{\Gamma_D}}{\varepsilon}\Big) \Bigg(\int_0^{d_{\Gamma_D}(x)} \Pi^{\partial\Omega}_{\sigma_x(t)}(\sigma'_x(t), \sigma'_x(t))\, (\theta \cdot n)(\sigma_x(t))\, dt \Bigg) \\
&u_{\Omega,\varepsilon} p_{\Omega,\varepsilon}\, ds(x),
\end{aligned} \tag{4.7}$$

where $\sigma_x(t) = exp_{p_{\Sigma_D}(x)}(t n_{\Sigma_D}(p_{\Sigma_D}(x)))$ is the unique geodesic passing through x and $p_{\Sigma_D}(x)$, and the adjoint state $p_{\Omega,\varepsilon}$ is the unique solution in $H^1(\Omega)$ to the following system:

$$\begin{cases} -\Delta p_{\Omega,\varepsilon} = -j(u_{\Omega,\varepsilon}) & \text{in } \Omega, \\ \frac{\partial p_{\Omega,\varepsilon}}{\partial n} + h_\varepsilon p_{\Omega,\varepsilon} = 0 & \text{on } \Gamma_D \cup \Gamma, \\ \frac{\partial p_{\Omega,\varepsilon}}{\partial n} = 0 & \text{on } \Gamma_N. \end{cases} \tag{4.8}$$

Equivalently, this rewrites (surface form):

$$
\begin{aligned}
J'_\varepsilon(\Omega)(\theta) = \int_{\Gamma\cup\Gamma_D} \Big(& j(u_{\Omega,\varepsilon}) - f p_{\Omega,\varepsilon} + \nabla_{\partial\Omega} u_{\Omega,\varepsilon} \cdot \nabla_{\partial\Omega} p_{\Omega,\varepsilon} \\
& - \frac{\partial u_{\Omega,\varepsilon}}{\partial n} \frac{\partial p_{\Omega,\varepsilon}}{\partial n} - \kappa\, p_{\Omega,\varepsilon} \frac{\partial u_{\Omega,\varepsilon}}{\partial n} \Big) \theta \cdot n \, ds \\
& + \frac{1}{\varepsilon^2} \int_{\Gamma\cup\Gamma_D} h'\Big(\frac{d_{\Gamma_D}}{\varepsilon}\Big) \Big(- \theta(p_{\Sigma_D}(x)) \cdot n_{\Sigma_D}(p_{\Sigma_D}(x)) \\
& + \int_0^{d_{\Gamma_D}(x)} \Pi^{\partial\Omega}_{\sigma_x(t)}(\sigma'_x(t), \sigma'_x(t))\ (\theta \cdot n)(\sigma_x(t))\, dt \Big) \\
& u_{\Omega,\varepsilon} p_{\Omega,\varepsilon}\, ds(x).
\end{aligned} \tag{4.9}
$$

Proof *We start with the proof of* (4.7). The proof is very similar to that of the volumetric formula (3.1) in Proposition 3, and we only sketch the main ingredients. At first, using the implicit function theorem, one sees that the solution $u_{\Omega,\varepsilon}$ to (4.2) has a 'Lagrangian derivative' $\mathring{u}_{\Omega,\varepsilon}(\theta)$, which is the unique solution in $H^1(\Omega)$ to the following variational problem: for all $v \in H^1(\Omega)$,

$$
\begin{aligned}
& \int_\Omega \nabla \mathring{u}_{\Omega,\varepsilon}(\theta) \cdot \nabla v \, dx + \int_{\Gamma\cup\Gamma_D} h_\varepsilon(d_{\Gamma_D}) \mathring{u}_{\Omega,\varepsilon}(\theta) v \, ds \\
& \quad = \int_\Omega (\mathrm{div}(f\theta)v + (\nabla\theta + \nabla\theta^T - \mathrm{div}\theta \mathrm{I}) \nabla u_{\Omega,\varepsilon} \cdot \nabla v)\, dx \\
& \quad - \int_{\Gamma\cup\Gamma_D} (\mathrm{div}_{\partial\Omega}\theta)\, h_\varepsilon(d_{\Gamma_D}) u_{\Omega,\varepsilon} v \, ds \\
& \quad - \frac{1}{\varepsilon^2} \int_{\Gamma\cup\Gamma_D} h'\Big(\frac{d_{\Gamma_D}}{\varepsilon}\Big) \Big(-\theta(x) \cdot \frac{\log_x(p_{\Sigma_D}(x))}{d_{\Gamma_D}(x)} \\
& \quad - \theta(p_{\Sigma_D}(x)) \cdot n_{\Sigma_D}(p_{\Sigma_D}(x)) \Big) u_{\Omega,\varepsilon} v \, ds(x) \\
& \quad - \frac{1}{\varepsilon^2} \int_{\Gamma\cup\Gamma_D} h'\Big(\frac{d_{\Gamma_D}}{\varepsilon}\Big) \Big(\int_0^{d_{\Sigma_D}(x)} \Pi^{\partial\Omega}_{\gamma(t)}(\gamma'(t), \gamma'(t))\ (\theta \cdot n)(\gamma(t))\, dt \Big) \\
& u_{\Omega,\varepsilon} v \, ds(x),
\end{aligned} \tag{4.10}
$$

where we have used Proposition 5 for the 'Lagrangian' derivative of the geodesic distance.

On the other hand, using a change of variables yields:

$$
J_\varepsilon(\Omega_\theta) = \int_\Omega |\det(\mathrm{I} + \nabla\theta)|\, j(u_{\Omega_\theta,\varepsilon} \circ (\mathrm{Id} + \theta))\, dx,
$$

whence, differentiating with respect to θ and using the variational formulation for the adjoint system (4.8):

$$\begin{aligned} J'_\varepsilon(\Omega)(\theta) &= \int_\Omega \mathrm{div}\theta\, j(u_{\Omega,\varepsilon})\, dx + \int_\Omega j'(u_{\Omega,\varepsilon})\mathring{u}_{\Omega,\varepsilon}(\theta)\, dx, \\ &= \int_\Omega \mathrm{div}\theta\, j(u_{\Omega,\varepsilon})\, dx - \int_\Omega \nabla\mathring{u}_{\Omega,\varepsilon}(\theta)\cdot\nabla p_{\Omega,\varepsilon}\, dx \\ &\quad \int_{\Gamma\cup\Gamma_D} h_\varepsilon(d_{\Gamma_D})\mathring{u}_{\Omega,\varepsilon}(\theta)p_{\Omega,\varepsilon}\, ds, \end{aligned}$$

Combining this with (4.10) eventually yields the desired result.
Proof of (4.9): To simplify notations, until the end of the proof, we take the shortcuts $u \equiv u_{\Omega,\varepsilon}$ and $p \equiv p_{\Omega,\varepsilon}$. We decompose the volumetric expression (4.7) as:

$$J'_\varepsilon(\Omega)(\theta) = I_1(\theta) + I_2(\theta),$$

where

$$\begin{aligned} I_1(\theta) &= \int_{\partial\Omega} (j(u) - fp)\,\theta\cdot n\, ds - \int_\Omega j'(u)\nabla u\cdot\theta\, dx \\ &\quad + \int_\Omega (\mathrm{div}\theta \mathrm{I} - \nabla\theta - \nabla\theta^T)\nabla u\cdot\nabla p\, dx \\ &\quad + \int_{\Gamma\cup\Gamma_D} \mathrm{div}_{\partial\Omega}\theta\, h_{\Omega,\varepsilon} up\, ds + \int_\Omega f\nabla p\cdot\theta\, dx, \end{aligned}$$

and

$$\begin{aligned} I_2(\theta) &= \frac{1}{\varepsilon^2}\int_{\Gamma\cup\Gamma_D} h'\left(\frac{d_{\Gamma_D}}{\varepsilon}\right)\left(-\theta(x)\cdot\frac{\log_x(p_{\Sigma_D}(x))}{d_{\Gamma_D}(x)}\right. \\ &\quad \left.-\theta(p_{\Sigma_D}(x))\cdot n_{\Sigma_D}(p_{\Sigma_D}(x))\right) up\, ds(x) \\ &\quad + \frac{1}{\varepsilon^2}\int_{\Gamma\cup\Gamma_D} h'\left(\frac{d_{\Gamma_D}}{\varepsilon}\right)\left(\int_0^{d_{\Gamma_D}(x)} \Pi^{\partial\Omega}_{\sigma_x(t)}\right. \\ &\quad \left.(\sigma'_x(t),\sigma'_x(t))\,(\theta\cdot n)(\sigma_x(t))\, dt\right) up\, ds(x). \end{aligned}$$

Let us first rearrange the expression of $I_1(\theta)$. To this end, using the same type of calculations as in the proofs of Proposition 2 and 3, integration by parts together with the fact that u and p have at least H^2 regularity near $\Gamma_D \cup \Gamma$ yield straightforwardly:

$$
\begin{aligned}
I_1(\theta) = &\int_{\partial\Omega} (j(u) - fp)\,\theta\cdot n\,ds - \int_\Omega j'(u)\nabla u\cdot\theta\,dx + \int_\Omega f\nabla p\cdot\theta\,dx \\
&+ \int_{\Gamma\cup\Gamma_D} \mathrm{div}_{\partial\Omega}\theta\, h_{\Omega,\varepsilon} up\,ds \\
&+ \int_{\Gamma\cup\Gamma_D} \left(\nabla u\cdot\nabla p\,\theta\cdot n - \frac{\partial u}{\partial n}\nabla p\cdot\theta - \frac{\partial p}{\partial n}\nabla u\cdot\theta\right) ds \\
&+ \int_\Omega (-\nabla(\nabla u\cdot\nabla p) + \Delta u\nabla p + \Delta p\nabla u + \nabla^2 p\nabla u + \nabla^2 u\nabla p)\cdot\theta\,dx \\
= &\int_{\partial\Omega} (j(u) - fp)\,\theta\cdot n\,ds + \int_{\Gamma\cup\Gamma_D} \mathrm{div}_{\partial\Omega}\theta\, h_{\Omega,\varepsilon} up\,ds \\
&+ \int_{\Gamma\cup\Gamma_D} \left(\nabla u\cdot\nabla p\,\theta\cdot n - \frac{\partial u}{\partial n}\nabla p\cdot\theta - \frac{\partial p}{\partial n}\nabla u\cdot\theta\right) ds.
\end{aligned}
\tag{4.11}
$$

Denoting by $\mathcal{D}$ the last integrand in the above right-hand side, we obtain:

$$
\begin{aligned}
\mathcal{D} &:= \nabla u\cdot\nabla p\,\theta\cdot n - \tfrac{\partial u}{\partial n}\nabla p\cdot\theta - \tfrac{\partial p}{\partial n}\nabla u\cdot\theta, \\
&= -\tfrac{\partial u}{\partial n}\tfrac{\partial p}{\partial n}\theta\cdot n - \left(\tfrac{\partial u}{\partial n}\nabla_{\partial\Omega} p\cdot\theta + \tfrac{\partial p}{\partial n}\nabla_{\partial\Omega} u\cdot\theta\right), \\
&= -\tfrac{\partial u}{\partial n}\tfrac{\partial p}{\partial n}\theta\cdot n + h_\varepsilon\left(u\nabla_{\partial\Omega} p\cdot\theta + p\nabla_{\partial\Omega} u\cdot\theta\right).
\end{aligned}
\tag{4.12}
$$

On the other hand, integrating by parts on the surface $\partial\Omega$ (see again Proposition 7), we obtain:

$$
\begin{aligned}
\int_{\partial\Omega} \mathrm{div}_{\partial\Omega}\theta\, h_{\Omega,\varepsilon} up\,ds = &\int_{\Gamma_D\cup\Gamma} h_\varepsilon\kappa up\theta\cdot n\,ds \\
&- \int_{\Gamma\cup\Gamma_D} h_\varepsilon(p\nabla_{\partial\Omega} u\cdot\theta + u\nabla_{\partial\Omega} p\cdot\theta)\,ds \\
&- \frac{1}{\varepsilon^2}\int_{\Gamma\cup\Gamma_D} h'(\frac{d_{\Gamma_D}}{\varepsilon})(\nabla_{\partial\Omega} d_{\Gamma_D}\cdot\theta) up\,ds.
\end{aligned}
\tag{4.13}
$$

Finally, combining (4.11) to (4.13) with the definitions of $I_1(\theta)$ and $I_2(\theta)$, as well as Proposition 4 for the tangential gradient of the geodesic signed distance function, the desired result follows. □

4.4 Study of the convergence of the approximate model to the exact problem

In this section, we are interested in evaluating in which capacity the exact shape optimization problem (2.4) is correctly approximated by its smoothed counterpart (4.6). More precisely, we investigate the convergence of the objective function $J_\varepsilon(\Omega)$ and that of its shape derivative $J'_\varepsilon(\Omega)$ to the exact versions $J(\Omega)$ and $J'(\Omega)$ respectively, for a fixed shape $\Omega\subset\mathbb{R}^2$. In order to keep the exposition as simple as possible, we proceed under the assumption (2.3), however we believe the result holds in greater generality, and notably in the 2d case where $\partial\Omega$ is not flat in the neighborhood of Σ_D; see Remark 4. Let us mention that a quite similar problem is investigated from

the theoretical viewpoint in [17], with stronger conclusions. Our first result in this direction is the following:

Theorem 2 *Under assumption (2.3), the function $u_{\Omega,\varepsilon}$ converges to u_Ω strongly in $H^1(\Omega)$, and the following estimate holds:*

$$||u_{\Omega,\varepsilon} - u_\Omega||_{H^1(\Omega)} \leq C_s \varepsilon^s ||f||_{L^2(\Omega)}, \tag{4.14}$$

for any $0 < s < \frac{1}{4}$, where the constant C_s depends on s.

Proof The error $r_\varepsilon := u_{\Omega,\varepsilon} - u_\Omega$ is the unique solution in $H^1(\Omega)$ to the system:

$$\begin{cases} -\Delta r_\varepsilon = 0 & \text{in } \Omega, \\ \frac{\partial r_\varepsilon}{\partial n} + h_\varepsilon r_\varepsilon = -\frac{\partial u_\Omega}{\partial n} - h_\varepsilon u_\Omega & \text{on } \partial\Omega, \end{cases} \tag{4.15}$$

which rewrites, under variational form:

$$\begin{aligned} \forall v \in H^1(\Omega), \quad & \int_\Omega \nabla r_\varepsilon \cdot \nabla v \, dx + \int_{\partial\Omega} h_\varepsilon r_\varepsilon v \, ds \\ & = -\int_{\partial\Omega} \frac{\partial u_\Omega}{\partial n} v \, ds - \int_{\Gamma_D \cup \Gamma} h_\varepsilon u_\Omega v \, ds. \end{aligned} \tag{4.16}$$

Note that the above variational problem is well-posed, as follows from the Lax-Milgram lemma and the following Poincaré-like inequality (which is proved by the standard contradiction argument):

$$\forall v \in H^1(\Omega), \quad ||v||^2_{H^1(\Omega)} \leq C \left(\int_\Omega |\nabla v|^2 \, dx + \int_{\Gamma_D} v^2 \, ds \right); \tag{4.17}$$

here and throughout the proof, C stands for a positive constant which is independent of ε. The estimate (4.14) is then obtained within two steps.

Step 1: We prove that r_ε is bounded in $H^1(\Omega)$, uniformly with respect to ε.

To this end, we estimate the first term in the right-hand side of (4.16) as:

$$\left| \int_{\partial\Omega} \frac{\partial u_\Omega}{\partial n} v \, ds \right| \leq C \left| \left| \frac{\partial u_\Omega}{\partial n} \right| \right|_{H^{-1/2}(\partial\Omega)} ||v||_{H^1(\Omega)}, \tag{4.18}$$

where we have the control

$$\left| \left| \frac{\partial u_\Omega}{\partial n} \right| \right|_{H^{-1/2}(\partial\Omega)} \leq C ||f||_{L^2(\mathbb{R}^d)},$$

as follows from the Green's formula (3.6) applied to the function u_Ω in $E(\Delta, L^2(\Omega))$ (see (3.5)). We are thus left with the task of estimating the second term in the right-hand side of (4.16), that is, the integral:

$$\int_{\Gamma_D \cup \Gamma} h_\varepsilon u_\Omega v \, ds = \int_\Gamma h_\varepsilon u_\Omega v \, ds.$$

To achieve this goal, recall that, since $u_\Omega \in H^s(\Omega)$ for $\frac{1}{2} < s < \frac{3}{2}$, and owing to the continuity of the trace $u \mapsto u|_{\partial\Omega}$ from $H^s(\Omega)$ into $H^{s-\frac{1}{2}}(\partial\Omega)$, for $s > \frac{1}{2}$ (see e.g. [44], Th. 3.37), it comes that $u_\Omega \in H^{s-\frac{1}{2}}(\partial\Omega)$, and in fact, using (2.2), that $u_\Omega \in \widetilde{H}^{s-\frac{1}{2}}(\Gamma_N \cup \Gamma)$. Using now the characterization (2.10) of the space $\widetilde{H}^{s-\frac{1}{2}}(\Gamma_N \cup \Gamma)$, it follows that for all $0 < \sigma < 1$, the function $\frac{1}{\rho^\sigma} u_\Omega$ belongs to $L^2(\Gamma)$, where we have introduced the weight $\rho(x) := \min(|x - s_0|, |x - s_1|)$.

Using this fact in combination with the Sobolev embedding from $H^{1/2}(\Gamma)$ into $L^q(\Gamma)$ for any $1 \leq q < \infty$ (see e.g. [1]), we get successively:

$$\begin{aligned}
\left| \int_\Gamma h_\varepsilon u_\Omega v \, ds \right| &= \left| \int_\Gamma \rho^\sigma h_\varepsilon \frac{1}{\rho^\sigma} u_\Omega v \, ds \right|, \\
&\leq \left(\int_\Gamma \rho^{p\sigma} h_\varepsilon^p \, ds \right)^{\frac{1}{p}} \left(\int_\Gamma \frac{1}{\rho^{2\sigma}} u_\Omega^2 \, ds \right)^{\frac{1}{2}} \left(\int_\Gamma v^q \, ds \right)^{\frac{1}{q}}, \\
&\leq \left(\int_\Gamma \rho^{p\sigma} h_\varepsilon^p \, ds \right)^{\frac{1}{p}} ||u_\Omega||_{\widetilde{H}^\sigma(\Gamma_N \cup \Gamma)} ||v||_{L^q(\Gamma)}, \\
&\leq C \left(\int_\Gamma \rho^{p\sigma} h_\varepsilon^p \, ds \right)^{\frac{1}{p}} ||u_\Omega||_{\widetilde{H}^\sigma(\Gamma_N \cup \Gamma)} ||v||_{H^1(\Omega)},
\end{aligned} \tag{4.19}$$

for any $p > 2$ (the constant C depends on p), where we have used Hölder's inequality with $\frac{1}{2} + \frac{1}{p} + \frac{1}{q} = 1$ to pass from the first line to the second one.

To proceed further, let us decompose Γ as

$$\begin{aligned}
&\Gamma = \Gamma_\varepsilon \cup \overline{U_0} \cup \overline{U_1}, \text{ where } U_i := \{x \in \Gamma, \ \ |x - s_i| < \varepsilon\}, \text{ and } \Gamma_\varepsilon \\
&:= \{x \in \Gamma, \ \ \rho(x) > \varepsilon\}.
\end{aligned}$$

Taking advantage of the structure (4.3) of h_ε, the first integral in the right-hand side of (4.19) is of the form

$$\begin{aligned}
\int_\Gamma \rho^{p\sigma} h_\varepsilon^p \, ds &= \int_{U_1} \rho^{p\sigma} h_\varepsilon^p \, ds + \int_{U_2} \rho^{p\sigma} h_\varepsilon^p \, ds + \int_{\Gamma_\varepsilon} \rho^{p\sigma} h_\varepsilon^p \, ds \\
&\leq \frac{C}{\varepsilon^p} \int_0^\varepsilon t^{p\sigma} h(\frac{t}{\varepsilon})^p dt, \\
&\leq \frac{C\varepsilon^{p\sigma+1}}{\varepsilon^p} \int_0^1 t^{p\sigma} h(t)^p \, dt, \\
&\leq C\varepsilon^{p(\sigma-1)+1}.
\end{aligned}$$

Therefore,

$$\left(\int_\Gamma \rho^{p\sigma} h_\varepsilon^p \, ds \right)^{\frac{1}{p}} \leq C\varepsilon^{\sigma-1+\frac{1}{p}};$$

now, choosing $p > 2$ and $\sigma < 1$ adequately and using (4.19), (2.13) and (2.11), we have proved that, for all $s < \frac{1}{2}$, there exists a constant C_s:

$$\left| \int_\Gamma h_\varepsilon u_\Omega v \, ds \right| \leq C_s \varepsilon^s ||f||_{L^2(\mathbb{R}^d)} ||v||_{H^1(\Omega)}. \tag{4.20}$$

Eventually, taking $v = r_\varepsilon$ as a test function in (4.16), we obtain the standard a priori estimate for r_ε:

$$\int_\Omega |\nabla r_\varepsilon|^2 \, dx + \int_{\partial\Omega} h_\varepsilon r_\varepsilon^2 \, ds = -\int_{\partial\Omega} \frac{\partial u_\Omega}{\partial n} r_\varepsilon \, ds - \int_\Gamma h_\varepsilon u_\Omega r_\varepsilon \, ds. \tag{4.21}$$

Combining (4.21) with the estimates (4.18) and (4.20), the Poincaré inequality (4.17) and the fact that $h_\varepsilon \geq 1$ on Γ_D (see (4.4)), it follows that there exists a constant C, which does not depend on ε, such that:

$$||r_\varepsilon||_{H^1(\Omega)} \leq C ||f||_{L^2(\mathbb{R}^d)}. \tag{4.22}$$

Step 2: We now turn to the proof of (4.14) *so to speak.*

Multiplying both sides of (4.21) by ε and using (4.4), we obtain:

$$\begin{aligned} ||r_\varepsilon||^2_{L^2(\Gamma_D)} &\leq C\varepsilon \int_{\Gamma_D} h_\varepsilon r_\varepsilon^2 \, ds, \\ &\leq C\varepsilon \left(\int_\Omega |\nabla r_\varepsilon|^2 \, dx + \int_{\partial\Omega} h_\varepsilon r_\varepsilon^2 \, ds \right) \\ &\leq C\varepsilon \left| \int_{\partial\Omega} \frac{\partial u_\Omega}{\partial n} r_\varepsilon \, ds \right| + C\varepsilon \left| \int_\Gamma h_\varepsilon u_\Omega r_\varepsilon \, ds \right|, \\ &\leq C\varepsilon ||f||^2_{L^2(\mathbb{R}^d)}, \end{aligned} \tag{4.23}$$

where we have used the estimate (4.20) with $v = r_\varepsilon$ and the bound (4.22) over r_ε.

Interpolating between (4.22) and (4.23) (see for instance [40]), for all $0 \leq s \leq \frac{1}{2}$, $s = (1-t)0 + \frac{1}{2}t$, there exists a constant C_s such that:

$$||r_\varepsilon||_{H^s(\Gamma_D)} \leq C_s ||r_\varepsilon||^{1-t}_{L^2(\Gamma_D)} ||r_\varepsilon||^t_{H^{\frac{1}{2}}(\Gamma_D)} \leq C_s \varepsilon^{\frac{1}{2}-s} ||f||_{L^2(\mathbb{R}^d)}.$$

Now, since $u_\Omega \in H^s(\Omega)$ for $\frac{1}{2} < s < \frac{3}{2}$, it comes that $\frac{\partial u_\Omega}{\partial n} \in H^{s-\frac{3}{2}}(\partial\Omega)$ (see [16], Lemma 4.3), and so

$$\left| \int_{\Gamma_D} \frac{\partial u_\Omega}{\partial n} r_\varepsilon \, ds \right| \leq \left| \left| \frac{\partial u_\Omega}{\partial n} \right| \right|_{H^{s-\frac{3}{2}}(\Gamma_D)} ||r_\varepsilon||_{H^{\frac{3}{2}-s}(\Gamma_D)} \leq C_s \varepsilon^{s-1} ||f||^2_{L^2(\mathbb{R}^d)}, \tag{4.24}$$

for all $1 < s < \frac{3}{2}$. Returning to (4.21) and using (4.17), (4.20) and (4.24), we now see that, for any $s < \frac{1}{2}$ and $\sigma < \frac{1}{2}$, there exists a constant $C > 0$ (depending on s and σ) such that:

$$
\begin{aligned}
||r_\varepsilon||^2_{H^1(\Omega)} &\leq C\left(\int_\Omega |\nabla r_\varepsilon|^2\, ds + \int_{\Gamma_D} r_\varepsilon^2\, ds\right)\\
&\leq C\left(\varepsilon^s ||f||^2_{L^2(\mathbb{R}^d)} + \varepsilon^\sigma ||f||_{L^2(\mathbb{R}^d)} ||r_\varepsilon||_{H^1(\Omega)}\right),
\end{aligned}
$$

Hence (4.14) holds, and this terminates the proof. □

As a straightforward consequence of Theorem 2, we obtain:

Corollary 1 *Under assumption (2.3), for any given admissible shape $\Omega \in \mathcal{U}_{DN}$, the approximate shape functional $J_\varepsilon(\Omega)$ converges to its exact counterpart $J(\Omega)$.*

Let us now turn to the convergence of the derivative of $J_\varepsilon(\Omega)$.

Theorem 3 *Under Assumption (2.3), for a given admissible shape $\Omega \in \mathcal{U}_{DN}$, the approximate shape derivative $J'_\varepsilon(\Omega)$ converges to its exact counterpart $J'(\Omega)$ in the sense that:*

$$
\sup_{\substack{\theta \in \Theta_{DN},\\ ||\theta||_{\Theta_{DN}} \leq 1}} |J'_\varepsilon(\Omega)(\theta) - J'(\Omega)(\theta)| = 0.
$$

Proof We rely on the volumetric expressions (3.13) and (4.7) of the shape derivatives $J'(\Omega)(\theta)$ and $J'_\varepsilon(\Omega)(\theta)$. In our context where (2.3) is satisfied, the boundary $\partial\Omega$ is flat in the neighborhood of $\Sigma_D = \{s_0, s_1\}$; hence, for $\varepsilon > 0$ small enough, the second fundamental form of $\partial\Omega$ vanishes where $h_\varepsilon > 0$, and the normal vectors $n_{\Sigma_D}(s_0)$, $n_{\Sigma_D}(s_1)$ to Σ_D coincide with the tangent vectors $\pm\tau(s_0)$ and $\pm\tau(s_1)$ to $\partial\Omega$. Then, the approximate shape derivative $J'_\varepsilon(\Omega)$ supplied by Proposition 6 simply boils down to:

$$
\begin{aligned}
J'(\Omega)(\theta) = &\int_{\partial\Omega} (j(u_{\Omega,\varepsilon}) - f p_{\Omega,\varepsilon})\, \theta \cdot n\, ds - \int_\Omega j'(u_{\Omega,\varepsilon}) \nabla u_{\Omega,\varepsilon} \cdot \theta\, dx\\
&+ \int_\Omega (\mathrm{div}\theta \mathrm{I} - \nabla\theta - \nabla\theta^T) \nabla u_{\Omega,\varepsilon} \cdot \nabla p_{\Omega,\varepsilon}\, dx\\
&+ \int_{\Gamma\cup\Gamma_D} \mathrm{div}_{\partial\Omega}\theta\, h_\varepsilon u_{\Omega,\varepsilon} p_{\Omega,\varepsilon}\, ds\\
&+ \frac{1}{\varepsilon^2}\int_{\Gamma\cup\Gamma_D} h'\left(\frac{x - s_0}{\varepsilon}\right)(\theta(x) - \theta(s_0)) \cdot n_{\Sigma_D}(s_0)\, u_{\Omega,\varepsilon} p_{\Omega,\varepsilon}\, ds(x)\\
&+ \frac{1}{\varepsilon^2}\int_{\Gamma\cup\Gamma_D} h'\left(\frac{x - s_1}{\varepsilon}\right)(\theta(x) - \theta(s_1)) \cdot n_{\Sigma_D}(s_1)\, u_{\Omega,\varepsilon} p_{\Omega,\varepsilon}\, ds(x)\\
&+ \int_\Omega f \nabla p_{\Omega,\varepsilon} \cdot \theta\, dx. \qquad (4.25)
\end{aligned}
$$

Given the expression (3.13) of the exact shape derivative $J'(\Omega)$, and in light of Theorem 2, it is obviously enough to show that the three integrals

$$
I_1(\theta) := \int_{\Gamma\cup\Gamma_D} \mathrm{div}_\Gamma\theta\, h_\varepsilon u_{\Omega,\varepsilon} p_{\Omega,\varepsilon}\, ds,
$$

$$I_2(\theta) := \frac{1}{\varepsilon^2}\int_{\Gamma\cup\Gamma_D} h'(\frac{x-s_0}{\varepsilon})(\theta(x)-\theta(s_0))\cdot\tau(s_0)u_{\Omega,\varepsilon}\,p_{\Omega,\varepsilon}\,ds(x),$$

and

$$I_3(\theta) := \frac{1}{\varepsilon^2}\int_{\Gamma\cup\Gamma_D} h'(\frac{x-s_1}{\varepsilon})(\theta(x)-\theta(s_1))\cdot\tau(s_1)\,u_{\Omega,\varepsilon}\,p_{\Omega,\varepsilon}\,ds(x)$$

converge to 0 as $\varepsilon\to 0$, uniformly with respect to θ when $||\theta||_{\Theta_{\rm DN}}\leq 1$.

As far as the integral $I_1(\theta)$ is concerned, Theorem 2 and the facts that $-\Delta u_\varepsilon = -\Delta u_\Omega = f$ imply that

$$\frac{\partial u_{\Omega,\varepsilon}}{\partial n}\to\frac{\partial u_\Omega}{\partial n}\ \text{in}\ H^{-1/2}(\partial\Omega),\ \text{and}\ u_{\Omega,\varepsilon}\to u_\Omega\ \text{in}\ H^{1/2}(\partial\Omega)\ \text{as}\ \varepsilon\to 0;$$

similar convergence results hold about $p_{\Omega,\varepsilon}$ and p_Ω. Therefore,

$$\int_{\Gamma\cup\Gamma_D}\mathrm{div}_\Gamma\theta\ h_{\Omega,\varepsilon}u_{\Omega,\varepsilon}p_{\Omega,\varepsilon}\,ds\xrightarrow{\varepsilon\to 0}-\int_{\Gamma\cup\Gamma_D}\mathrm{div}_\Gamma\theta\,\frac{\partial u_\Omega}{\partial n}p_\Omega\,ds,\qquad(4.26)$$

where the last integral may be decomposed as

$$\int_{\Gamma\cup\Gamma_D}\mathrm{div}_{\partial\Omega}\theta\,\frac{\partial u_\Omega}{\partial n}p_\Omega\,ds=\int_{\Gamma_D}\mathrm{div}_{\partial\Omega}\theta\,\frac{\partial u_\Omega}{\partial n}p_\Omega\,ds+\int_\Gamma\mathrm{div}_{\partial\Omega}\theta\,\frac{\partial u_\Omega}{\partial n}p_\Omega\,ds=0,$$

as follows from the boundary conditions satisfied by u_Ω and p_Ω. This convergence is easily seen to be uniform with respect to $\theta\in\Theta_{\rm DN}$, $||\theta||_{\Theta_{\rm DN}}\leq 1$.

Let us now turn to the treatment of $I_2(\theta)$, that of $I_3(\theta)$ being on all points identical. We assume for notation simplicity that $s_0=0$, and again, we identify the neighborhood of s_0 in $\partial\Omega$ (which is a horizontal line) with a subset of the real line $\mathbb{R}$. The key remark in the analysis of $I_2(\theta)$ is that there exists a vector field $\widetilde{\theta}(x)$ vanishing identically on Γ_N such that $(\theta(x)-\theta(0))\cdot\tau(0)=x\cdot\tilde{\theta}(x)$, as is easily seen from a Taylor expansion at 0. This will allow to improve the available convergence rates of $u_{\Omega,\varepsilon}$ and $p_{\Omega,\varepsilon}$ in the integrand of $I_2(\theta)$. More precisely, using integration by parts on the boundary $\partial\Omega$, $I_2(\theta)$ rewrites:

$$\begin{aligned}
I_2(\theta) &= \int_{\Gamma\cup\Gamma_D}\frac{\partial h_\varepsilon}{\partial\tau}x\cdot\tilde{\theta}(x)u_{\Omega,\varepsilon}p_{\Omega,\varepsilon}\,ds,\\
&= -\int_{\Gamma\cup\Gamma_D}h_\varepsilon\frac{\partial}{\partial\tau}\left(x\cdot\tilde{\theta}(x)u_{\Omega,\varepsilon}p_{\Omega,\varepsilon}\right)ds,\\
&= -\int_{\Gamma\cup\Gamma_D}h_\varepsilon\tilde{\theta}(x)\cdot\left(x\frac{\partial u_{\Omega,\varepsilon}}{\partial\tau}p_{\Omega,\varepsilon}+x\frac{\partial p_{\Omega,\varepsilon}}{\partial\tau}u_{\Omega,\varepsilon}\right)ds\\
&\quad-\int_{\Gamma\cup\Gamma_D}h_\varepsilon u_{\Omega,\varepsilon}p_{\Omega,\varepsilon}\frac{\partial(x\cdot\tilde{\theta}(x))}{\partial\tau}\,ds\\
&= -\int_{\Gamma\cup\Gamma_D}h_\varepsilon\tilde{\theta}(x)\cdot\left(x\frac{\partial u_{\Omega,\varepsilon}}{\partial\tau}p_{\Omega,\varepsilon}+x\frac{\partial p_{\Omega,\varepsilon}}{\partial\tau}u_{\Omega,\varepsilon}\right)ds+R_\varepsilon(\theta),
\end{aligned}$$

where $R_\varepsilon(\theta)$ is a remainder (possibly changing from one line to the next) gathering several integrals which are proved to converge to 0 as $\varepsilon \to 0$, uniformly with respect to θ when $||\theta||_{\Theta_{\mathrm{DN}}} \leq 1$ owing to similar calculations to those involved in the above proof of convergence of $I_1(\theta)$ (see (4.26)). Then, using the boundary conditions satisfied by $u_{\Omega,\varepsilon}$ and $p_{\Omega,\varepsilon}$,

$$\begin{aligned} I_2(\theta) &= \int_{\Gamma\cup\Gamma_D} \left(\rho(x)\frac{\partial u_{\Omega,\varepsilon}}{\partial\tau}\frac{\partial p_{\Omega,\varepsilon}}{\partial n} + \rho(x)\frac{\partial p_{\Omega,\varepsilon}}{\partial\tau}\frac{\partial u_{\Omega,\varepsilon}}{\partial n}\right)\left(\frac{x}{\rho(x)}\cdot\tilde{\theta}(x)\right) ds + R_\varepsilon(\theta), \\ &= \int_{\Gamma\cup\Gamma_D} \left(\frac{\partial(\rho u_{\Omega,\varepsilon})}{\partial\tau}\frac{\partial p_{\Omega,\varepsilon}}{\partial n} + \frac{\partial(\rho p_{\Omega,\varepsilon})}{\partial\tau}\frac{\partial u_{\Omega,\varepsilon}}{\partial n}\right)\left(\frac{x}{\rho(x)}\cdot\tilde{\theta}(x)\right) ds + R_\varepsilon(\theta), \end{aligned}$$

where we have posed $\rho(x) = |x|$ and the same calculations as in (4.26) have been used.

At this point, we know from Theorem 2 that $\frac{\partial u_{\Omega,\varepsilon}}{\partial n}$ (resp. $\frac{\partial p_{\Omega,\varepsilon}}{\partial n}$) converges to $\frac{\partial u_\Omega}{\partial n}$ (resp. $\frac{\partial p_\Omega}{\partial n}$) in $H^{-1/2}(\partial\Omega)$. Hence, the proof of the convergence of $I_2(\theta)$, and thereby that of Theorem 3, follows from the following results:

$$\frac{\partial(\rho u_{\Omega,\varepsilon})}{\partial\tau} \xrightarrow{\varepsilon\to 0} \frac{\partial(\rho u_\Omega)}{\partial\tau} \text{ in } H^1(\Omega), \text{ and } \frac{\partial(\rho p_{\Omega,\varepsilon})}{\partial\tau} \xrightarrow{\varepsilon\to 0} \frac{\partial(\rho p_\Omega)}{\partial\tau} \text{ in } H^1(\Omega), \tag{4.27}$$

where τ stands for any smooth extension to the whole Ω of the tangent vector τ to $\partial\Omega$; see Appendix A. We now sketch the proof of this last statement focusing on the case of $u_{\Omega,\varepsilon}$; the counterpart result as regards $p_{\Omega,\varepsilon}$ being proved in a similar fashion.

The convergence (4.27) actually follows from exactly the same arguments as that in the proof of (4.14). At first, using the representation of Proposition 1 (or more exactly a higher-order avatar of it, see Remark 3), observe that the function ρu_Ω belongs to $H^s(\Omega)$ for all $0 \leq s < \frac{5}{2}$. Letting the notation $r_\varepsilon := u_{\Omega,\varepsilon} - u_\Omega$, and using test functions of the form $\rho(x)v \in H^1(\Omega)$ for $v \in H^1(\Omega)$ inside the variational formulation (4.16) of r_ε, we see that ρr_ε satisfies:

$$\begin{aligned} &\forall v \in H^1(\Omega), \quad \int_\Omega \nabla(\rho r_\varepsilon)\cdot\nabla v\, dx + \int_{\Gamma\cup\Gamma_D} h_\varepsilon \rho r_\varepsilon v\, ds \\ &= -\int_\Gamma h_\varepsilon \rho u_\Omega v\, ds - \int_{\Gamma_D} \frac{\partial u_\Omega}{\partial n}\rho v\, ds - \int_\Omega \nabla\rho\cdot(v\nabla r_\varepsilon - r_\varepsilon\nabla v)\, dx. \end{aligned} \tag{4.28}$$

Now using test functions of the form $\frac{\partial v}{\partial\tau}$, $v \in H^1(\Omega)$ in (4.28),

then integrating by parts yields the following variational formulation for $q_\varepsilon := \frac{\partial(\rho r_\varepsilon)}{\partial\tau}$:

$$\begin{aligned} &\forall v \in H^1(\Omega), \quad -\int_\Omega \nabla q_\varepsilon\cdot\nabla v\, dx - \int_{\Gamma\cup\Gamma_D} h_\varepsilon q_\varepsilon v\, ds = \int_{\partial\Omega} \frac{\partial h_\varepsilon}{\partial\tau}\rho r_\varepsilon v\, ds \\ &\quad + \int_\Gamma \frac{\partial}{\partial\tau}(h_\varepsilon\rho(x)u_\Omega)v\, ds + \int_{\Gamma_D}\frac{\partial}{\partial\tau}\left(\rho\frac{\partial u_\Omega}{\partial n}\right)v\, ds \\ &\quad + \langle F_\varepsilon, v\rangle_{H^1(\Omega)^*, H^1(\Omega)}, \end{aligned} \tag{4.29}$$

where the remainder F_ε is a sequence of linear forms in the dual $H^1(\Omega)^*$ of $H^1(\Omega)$ which converges to 0 in the strong dual topology.

Finally, using the result of Theorem 2, together with very similar calculations than those involved in its proof, the desired result (4.27) follows, which concludes the proof. □

5 Numerical illustrations

In this final section we present several numerical illustrations of the previous mathematical developments. The examples discussed below take place in situations which are variations of the basic model introduced in Sect. 2.1. The notations may differ slightly depending on the context at stake, and so do the involved numerical methods; the precise description of the considered setting is adapted to each particular case.

One common feature of our examples is that all of the simulations are done using the finite element method in `FreeFem++` [32] with Lagrange $\mathbb{P}_1$ finite elements. When it comes to operations related to the level set method we used our own `C++` implementation interfaced within `FreeFem++`. Finally, all computations were done on a basic laptop.

We start in Sect. 5.1 with a fairly simple academic example which aims to validate the approximation procedure of Sect. 4 for optimization problems featuring the transition between regions supporting homogeneous Dirichlet and Neumann boundary conditions. We then turn in Sects. 5.2 and 5.3 to more realistic applications in the context of the linearized elasticity equations. Specifically, Sect. 5.3 deals with problems where both the shape and the region of its boundary supporting Dirichlet boundary conditions are subject to optimization.

5.1 An academic, validation example

We start with a toy example, meant to assess the validity of the approximation process of Sect. 4 for the optimization of the transition Σ_D between regions of the shape Ω bearing homogeneous Dirichlet and Neumann boundary conditions.

We consider a rectangular domain $\Omega = (-1, 1) \times (-\frac{1}{2}, \frac{1}{2})$, as depicted on Fig. 4 (left), which is filled with a material with inhomogeneous conductivity $a \in L^\infty(\Omega)$ satisfying the conditions

$$m \leq a(x) \leq M \text{ a.e. } x \in \Omega,$$

for some constants $0 < m \leq M$. To be quite precise, in the present application, $a(x)$ takes the values 1 inside a (fixed) subset $K \subset \Omega$, and 100 outside K. A constant, unit body source is acting inside Ω, and the boundary $\partial\Omega$ is divided into two distinct regions Γ_D and Γ supporting respectively homogeneous Dirichlet and Neumann boundary conditions. The region Γ_D is parametrized by two real parameters α, β, and is thenceforth denoted by $\Gamma_{\alpha,\beta}$; it is of the form:

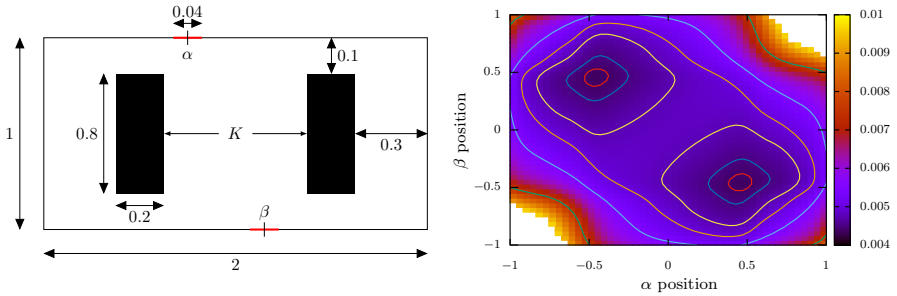

Fig. 4 (Left) Setting of the validation example of Sect. 5.1; (right) value of the objective function for all admissible positions of the boundary Γ_D, parametrized by α and β

$$\Gamma_{\alpha,\beta} = \left\{\left(\alpha + t, -\frac{1}{2}\right),\ t \in (-w, w)\right\} \cup \left\{\left(\beta + t, \frac{1}{2}\right),\ t \in (-w, w)\right\}; \quad (5.1)$$

in other terms, $\Gamma_{\alpha,\beta}$ is the reunion of two intervals with fixed width $w > 0$, which are respectively centered at the points $(\alpha, -\frac{1}{2})$ and $(\beta, \frac{1}{2}) \in \partial\Omega$, where $\alpha, \beta \in (-1 + w, 1 - w)$. In this situation, the voltage potential $u_{\alpha,\beta}$ inside Ω arises as the unique solution in $H^1_{\Gamma_{\alpha,\beta}}(\Omega)$ to the conductivity equation:

$$\begin{cases} -\mathrm{div}(a(x)\nabla u_{\alpha,\beta}) = 1 \text{ in } \Omega, \\ u_{\alpha,\beta} = 0 \qquad \text{on } \Gamma_{\alpha,\beta}, \\ \frac{\partial u_{\alpha,\beta}}{\partial n} = 0 \qquad \text{on } \Gamma. \end{cases} \quad (5.2)$$

Our purpose is to optimize the position (α, β) of the two intervals defining $\Gamma_{\alpha,\beta}$ so as to minimize the average potential inside the region K; that is, we considered the following optimization problem of two real parameters:

$$\inf_{(\alpha,\beta)\in(-1+w,1-w)^2} J(\alpha, \beta), \text{ where } J(\alpha, \beta) := \int_K u_{\alpha,\beta}\, dx. \quad (5.3)$$

We first perform a brute-force calculation of all the possible values $J(\Omega)$ when the couple (α, β) runs through the set $(-1 + w, 1 - w)^2$. The results are reported on Fig. 4. In particular, it is visible that $J(\alpha, \beta)$ possesses two local minima, near the points $(-0.5, 0.5)$ and $(0.5, -0.5)$, respectively.

According to the methodology developed in Sect. 4, we now approximate the problem (5.3) by that

$$\inf_{(\alpha,\beta)\in(-1+w,1-w)^2} J_\varepsilon(\alpha, \beta), \text{ where } J_\varepsilon(\alpha, \beta) := \int_K u_{\alpha,\beta,\varepsilon}\, dx, \quad (5.4)$$

featuring the solution $u_{\alpha,\beta,\varepsilon} \in H^1(\Omega)$ to the following smoothed counterpart of (5.2):

$$\begin{cases} -\mathrm{div}(a(x)\nabla u_{\alpha,\beta,\varepsilon}) = 1 \text{ in } \Omega, \\ \frac{\partial u_{\alpha,\beta,\varepsilon}}{\partial n} + h_\varepsilon u_{\alpha,\beta,\varepsilon} = 0 \text{ on } \partial\Omega. \end{cases} \quad (5.5)$$

In (5.5), the interpolation profile h_ε is constructed as in (4.3), in which the small parameter ε is chosen of the order of the mesh size.

The partial derivatives of $J_\varepsilon(\alpha, \beta)$ are easily calculated thanks to Proposition 6, taking advantage of the particularly simple form (5.1) of the optimized region Γ_D of $\partial\Omega$; for instance, one has:

$$\frac{\partial J_\varepsilon}{\partial\alpha}(\alpha,\beta) = -\frac{1}{\varepsilon^2}\int_{L_\alpha^+} h'\left(\frac{t-\alpha-w}{\varepsilon}\right) u_{\alpha,\beta,\varepsilon}\, p_{\alpha,\beta,\varepsilon}\, dt + \frac{1}{\varepsilon^2}\int_{L_\alpha^-} h'\left(\frac{-t+\alpha-w}{\varepsilon}\right) u_{\alpha,\beta,\varepsilon}\, p_{\alpha,\beta,\varepsilon}\, dt,$$

where L_α^+, L_α^- are the one-dimensional sets defined by $L_\alpha^+ = \left\{(t, -\frac{1}{2}),\ t > \alpha\right\}$, $L_\alpha^- = \left\{(t, -\frac{1}{2}),\ t < \alpha\right\}$ (with a little abuse of notations, $L_\alpha^\pm$ are identified to the corresponding subsets of the real line). In the above expression, the adjoint state $p_{\alpha,\beta,\varepsilon}$ is the unique solution in $H^1(\Omega)$ to the problem:

$$\begin{cases} -\mathrm{div}(a(x)\nabla p_{\alpha,\beta,\varepsilon}) = -\mathbb{1}_K \text{ in } \Omega, \\ \frac{\partial p_{\alpha,\beta,\varepsilon}}{\partial n} + h_\varepsilon\, p_{\alpha,\beta,\varepsilon} = 0 \quad \text{on } \partial\Omega, \end{cases}$$

where $\mathbb{1}_K$ is the characteristic function of K. A similar expression holds for the partial derivative $\frac{\partial J_\varepsilon}{\partial\beta}$.

We solve the approximate problem (5.4) by means of a standard gradient algorithm, starting from several different initial configurations (α, β) as regards the two connected components of $\Gamma_{\alpha,\beta}$. The results are reported in Fig. 5: in particular, depending on the initialization, the boundary $\Gamma_{\alpha,\beta}$ smoothly converges to an optimized position which matches the two local minima of the exact functional $J(\alpha, \beta)$ (see again Fig. 4, (right)). This indicates a good agreement between the exact optimization problem (5.3) and its approximation (5.4), and notably between the exact and approximate derivatives of the optimized criterion.

5.2 Optimization of the repartition of clamps and locators on the boundary of an elastic structure

Our second example deals with the application of the results of Sects. 3 and 4 to the problem of optimal repartition of clamps and locators on an elastic structure; see [11], Chap. 9, for a presentation of the physical context and [36,41,50] for optimization studies conducted in this context.

5.2.1 Description of the physical setting and of the optimization problem

In this example, Ω stands for a three-dimensional rectangular beam with size $4 \times 1 \times 1$, filled with a linearly elastic material, whose Hooke's law A is defined by, for any symmetric matrix e with size 3×3:

$$Ae = 2\mu e + \lambda \mathrm{tr}(e),$$

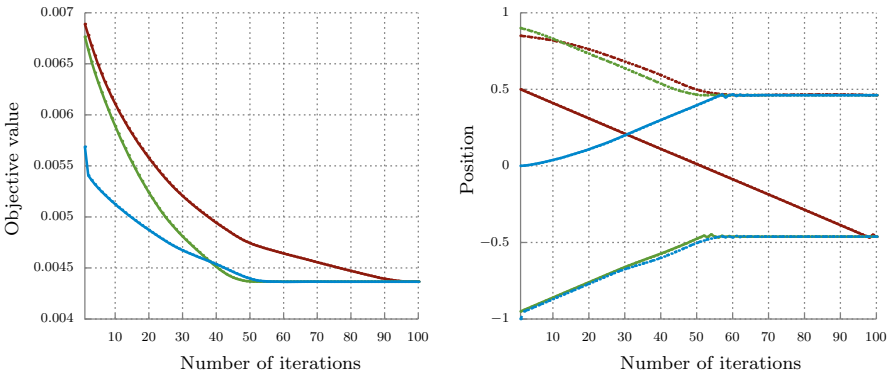

(a) *Convergence history of the objective function*

(b) *Successive values of α (solid lines) and β (dashed lines)*

Fig. 5 Histories of (left) the objective function $J_\varepsilon(\alpha, \beta)$ and (right) the locations α, β of the components of the optimized boundary $\Gamma_{\alpha,\beta}$ in the validation example of Sect. 5.1. Three experiments are performed, with different initial values (α, β) (associated to red, green and blue lines) (color figure online)

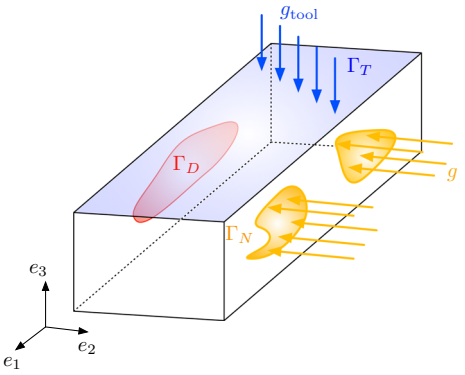

Fig. 6 Setting of the example of Sect. 5.2 about the optimal repartition of clamps and locators on the boundary of an elastic structure

where λ, μ are the Lamé parameters of the material; in our context

$$\lambda = \frac{E\nu}{(1+\nu)(1-2\nu)}, \quad \mu = \frac{E}{1+\nu} \tag{5.6}$$

with $E = 100$, $\nu = 0.3$. During its construction, Ω receives the vertical load $g_{\text{tool}} = (0, 0, -1)$ from the manufacturing tool, which is applied on the upper side Γ_T of its boundary. So that the structure do not move under this effort, a *clamping-locator* system is used: Ω is attached on a subregion Γ_D of the left-hand side Λ_D of $\partial\Omega$ (locator), while it receives a prescribed load $g = (0, -1, 0)$ on another region Γ_N of the right-hand side $\Lambda_N \subset \partial\Omega$ (clamping); the latter is exerted by an external mechanical device pressing against the structure; see Fig. 6 for a sketch of the situation.

In this context, the displacement of Ω is the unique solution $u_{\Gamma_D,\Gamma_N} \in H^1_{\Gamma_D}(\Omega)^3$ to the following linear elasticity system:

$$\begin{cases} -\mathrm{div}(Ae(u_{\Gamma_D,\Gamma_N}) = 0 \text{ in } \Omega, \\ u_{\Gamma_D,\Gamma_N} = 0 \quad \text{on } \Gamma_D, \\ Ae(u_{\Gamma_D,\Gamma_N})n = g_{\text{tool}} \quad \text{on } \Gamma_T, \\ Ae(u_{\Gamma_D,\Gamma_N})n = g \quad \text{on } \Gamma_N, \\ Ae(u_{\Gamma_D,\Gamma_N})n = 0 \quad \text{on } \Gamma, \end{cases} \tag{5.7}$$

where $e(u) := \frac{1}{2}(\nabla u + \nabla u^T)$ is the strain tensor associated to a vector field $u : \Omega \to \mathbb{R}^3$.

Our aim is to optimize the positions Γ_N and Γ_D of clamps and locators on the surface of the structure Ω, whose shape itself is not subject to optimization, so that the displacement of Ω under the action of g_{tool} be minimal. We also add constraints on the size of the regions Γ_N, Γ_D and on the perimeter of Γ_D via fixed penalizations of the objective function. More precisely, we consider the optimization problem:

$$\inf_{\substack{\Gamma_D \subset \Lambda_D \\ \Gamma_N \subset \Lambda_N}} J(\Gamma_D, \Gamma_N), \text{ where}$$
$$J(\Gamma_D, \Gamma_N) = \int_\Omega |u_{\Gamma_D,\Gamma_N}|^2 \, dx + \ell_D \int_{\Gamma_D} ds + \ell_N \int_{\Gamma_N} ds + \ell_{K_D} \int_{\Sigma_D} ds, \tag{5.8}$$

where ℓ_D, ℓ_N and ℓ_{K_D} are fixed Lagrange multipliers: $\ell_D = 2.10^{-2}$, $\ell_N = 10^{-3}$, $\ell_{K_D} = 10^{-2}$. In the framework of Hadamard's method (see Sect. 2.2), we consider deformations θ such that:

$$\theta \cdot n = 0 \text{ on } \partial\Omega, \text{ and } \theta = 0 \text{ on } \partial\Omega \setminus (\Lambda_D \cup \Lambda_N). \tag{5.9}$$

The numerical resolution of this problem relies on the knowledge of the shape derivatives of the partial mappings $\Gamma_D \mapsto J(\Gamma_D, \Gamma_N)$ and $\Gamma_N \mapsto J(\Gamma_D, \Gamma_N)$. In order to accomodate the presence of the transition $\Sigma_D := \overline{\Gamma_D} \cap \overline{\Gamma} \subset \Lambda_D$ between homogeneous Dirichlet and Neumann boundary conditions, we follow the lead of Sect. 4 and consider the following approximate counterpart of (5.10):

$$\inf_{\substack{\Gamma_D \subset \Lambda_D \\ \Gamma_N \subset \Lambda_N}} J_\varepsilon(\Gamma_D, \Gamma_N), \text{ where}$$
$$J_\varepsilon(\Gamma_D, \Gamma_N) := \int_\Omega |u_{\Gamma_D,\Gamma_N,\varepsilon}|^2 \, dx + \ell_D \int_{\Gamma_D} ds + \ell_N \int_{\Gamma_N} ds + \ell_{K_D} \int_{\Sigma_D} ds, \tag{5.10}$$

where $u_{\Gamma_D,\Gamma_N,\varepsilon}$ is the solution in $H^1(\Omega)^3$ to the system:

$$\begin{cases} -\mathrm{div}(Ae(u_{\Gamma_D,\Gamma_N,\varepsilon}) = 0 & \text{in } \Omega, \\ Ae(u_{\Gamma_D,\Gamma_N,\varepsilon}) + h_\varepsilon u_{\Gamma_D,\Gamma_N,\varepsilon} = 0 & \text{on } \Lambda_D, \\ Ae(u_{\Gamma_D,\Gamma_N,\varepsilon})n = g_{\text{tool}} & \text{on } \Gamma_T, \\ Ae(u_{\Gamma_D,\Gamma_N,\varepsilon})n = g & \text{on } \Gamma_N, \\ Ae(u_{\Gamma_D,\Gamma_N,\varepsilon})n = 0 & \text{on } \Gamma \setminus \Lambda_D, \end{cases} \tag{5.11}$$

featuring the interpolation profile h_ε in (4.3).

Thence, the calculation of the shape derivative of $\Gamma_N \mapsto J_\varepsilon(\Gamma_D, \Gamma_N)$ is provided by Sect. 3.1, or more exactly, the straightforward adaptation of its proof to the present linearized elasticity context. The shape derivative of the smoothed mapping $\Gamma_D \mapsto J_\varepsilon(\Gamma_D, \Gamma_N)$ is calculated exactly as in the proof of Proposition 6 (or by using Céa's formal method), and we omit the formula for brevity.

5.2.2 Numerical representation of the regions Γ_N and Γ_D

When it comes to the numerical representation of the optimized subsets Γ_D and Γ_N of the lateral boundaries Λ_D and $\Lambda_N \subset \partial\Omega$, we rely on the level set method, pioneered in [48], then introduced in the shape optimization context in [5,52,55].

Let us for instance provide a little more details about the numerical representation of Γ_D—the same ingredients being used in the case of Γ_N. The region Γ_D is described as the negative subdomain of a scalar 'level set' function $\phi : \Lambda_D \to \mathbb{R}$, defined on the (planar) lateral boundary Λ_D, that is:

$$\forall x \in \Lambda_D, \quad \begin{cases} \phi(x) < 0 \text{ if } x \in \Gamma_D, \\ \phi(x) = 0 \text{ if } x \in \Sigma_D, \\ \phi(x) > 0 \text{ otherwise.} \end{cases}$$

The motion in (pseudo) time of $\Gamma_D \equiv \Gamma_D(t)$ according to a velocity field with normal component $v(t,x)$ (which in our case is associated to the shape gradient of the optimized functional $J_\varepsilon(\Gamma_D, \Gamma_N)$ in (5.10)) is then described in terms of an associated level set function $\phi(t,\cdot)$ by the following Hamilton-Jacobi equation:

$$\frac{\partial \phi}{\partial t}(t,x) + v(t,x)|\nabla \phi(t,x)| = 0, \text{ for } t > 0, \ x \in \Lambda_D. \tag{5.12}$$

In practice, (5.12) is discretized in time, and solved on a Cartesian grid of Λ_D by means of the second-order scheme presented in [51], §6.4.

Last but not least, let us mention that at each iteration of the process, the level set function ϕ is reinitialized as the signed distance function d_{Γ_D} to the actual region Γ_D by using the fast marching algorithm (see for instance [51], Chap. 8). On the one hand, this operation is well-known to be a key ingredient in the numerical performance of the level set method (see again [51]); on the other hand, the signed distance function d_{Γ_D} is needed to calculate the coefficient h_ε in (5.11) (see again (4.3)).

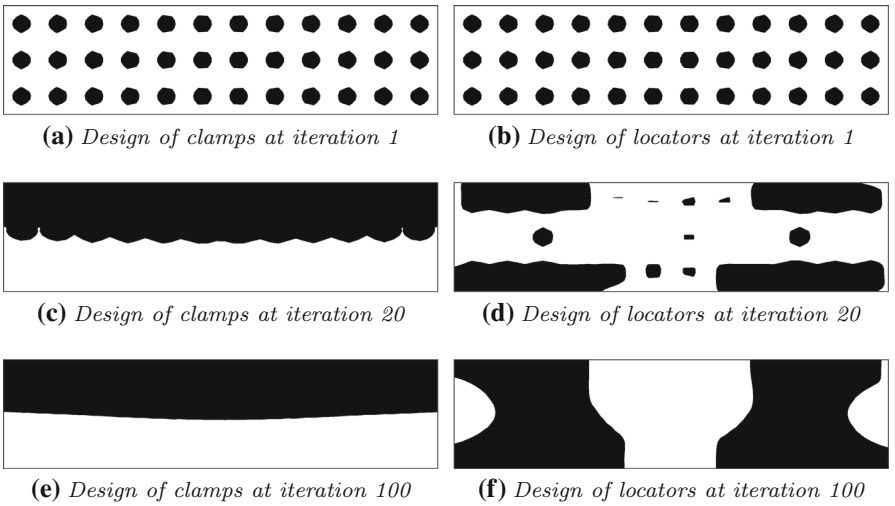

(a) *Design of clamps at iteration 1* **(b)** *Design of locators at iteration 1*

(c) *Design of clamps at iteration 20* **(d)** *Design of locators at iteration 20*

(e) *Design of clamps at iteration 100* **(f)** *Design of locators at iteration 100*

Fig. 7 Initial, intermediate and optimized designs of clamps and locators in the test-case of Sect. 5.2

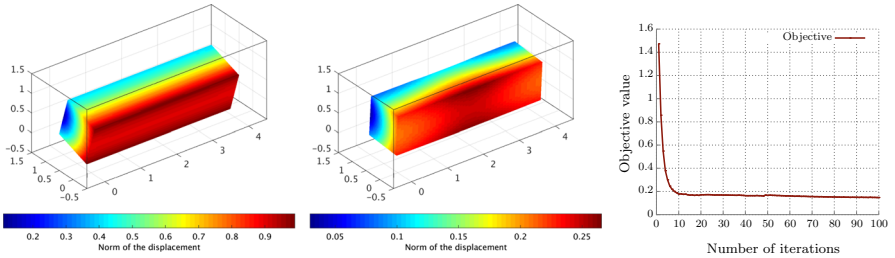

(a) *Deformed configuration of Ω with the initial configuration of clamps and locators*

(b) *Deformed configuration of Ω with the optimized configuration of clamps and locators*

(c) *Convergence history*

Fig. 8 Details of the optimization example of clamps and locators of Sect. 5.2

5.2.3 Numerical application

Let us now consider a concrete example in the previous context. A tetrahedral mesh of Ω composed of 45000 vertices is used, and the optimization problem (5.10) is solved for the positions of Γ_D and Γ_N while, again, the shape of Ω itself is unchanged. Relying on the level set method of Sect. 5.2.2 for representing Γ_D and Γ_N, we use a standard gradient algorithm based on the knowledge of the shape derivatives of $\Gamma_D \mapsto J_\varepsilon(\Gamma_D, \Gamma_N)$ and $\Gamma_N \mapsto J_\varepsilon(\Gamma_D, \Gamma_N)$; the computation takes about 8 hours and the results are presented on Fig. 7.

We notice in particular that the optimized design of the clamps is concentrated under Γ_T whereas the locators are symmetrically positioned at both ends of the beam. The deformed configurations of the initial and optimized shapes are displayed in Fig. 8.

5.3 Joint optimization of the shape and the regions supporting different types of boundary conditions

We finally turn to examples where the shape Ω of a 2d structure is optimized at the same time as the region Γ_D of its boundary supporting homogeneous Dirichlet boundary conditions. For simplicity, the region Γ_N supporting inhomogeneous Neumann boundary conditions is fixed, which means that we are exactly in the setting of Sects. 3.2 and 4: in all the examples in this subsection, we consider the following shape and topology optimization problem:

$$\inf_{\substack{\Omega \subset D \\ \Gamma_D \subset \Lambda_D \cap \partial\Omega}} J(\Omega), \text{ where } J(\Omega) = j(u_\Omega) + \ell_V \int_\Omega ds + \ell_D \int_{\Gamma_D} ds \tag{5.13}$$

is a weighted sum of a case-dependent objective defined from a smooth function j, involving the elastic displacement u_Ω of the shape, solution to (5.11), and of constraints on both the volume of shapes, and on the area of the Dirichlet boundary Γ_D (the latter constraints being enforced by means of fixed Lagrange multipliers ℓ_V, ℓ_D). Notice that in the statement (5.13) of the considered shape optimization problem, we have committed the same abuse of notations as in Sect. 2.2: u_Ω and $J(\Omega)$ depend on both the overall shape Ω of the structure and the position Γ_D of the region supporting homogeneous Dirichlet boundary conditions (the latter being constrained to belong to a fixed region Λ_D of the computational domain D), while only the first dependence is explicit.

As regards the numerical setting, the computational domain D is equipped with a fixed mesh. Each shape $\Omega \subset D$ is represented by the level set method, i.e. Ω is described via a level set function $\phi : D \to \mathbb{R}$ such that:

$$\forall x \in D, \quad \begin{cases} \phi(x) < 0 \text{ if } x \in \Omega, \\ \phi(x) = 0 \text{ if } x \in \partial\Omega, \\ \phi(x) > 0 \text{ otherwise;} \end{cases}$$

see Sect. 5.2.2 above for more details about the level set method.

Since the shape Ω is not discretized (it is only known via the datum of a level set function), no computational mesh is available to calculate the elastic displacement u_Ω by means of a standard finite element method. To alleviate this issue, the 'ersatz material trick' (see e.g. [3,5,12]) is used to approximate the considered linearized elasticity systems posed on Ω with systems posed on D as a whole: u_Ω is approximated by the solution u to:

$$\begin{cases} -\text{div}(A_\eta e(u)) = 0 \text{ in } D, \\ u = 0 \quad \text{on } \Gamma_D, \\ A_\eta e(u) n = g \quad \text{on } \Gamma_N, \\ A_\eta e(u) = 0 \quad \text{on } \Gamma, \end{cases} \text{ where } A_\eta(x) := \begin{cases} A \text{ if } x \in \Omega, \\ \eta A \text{ otherwise,} \end{cases}$$

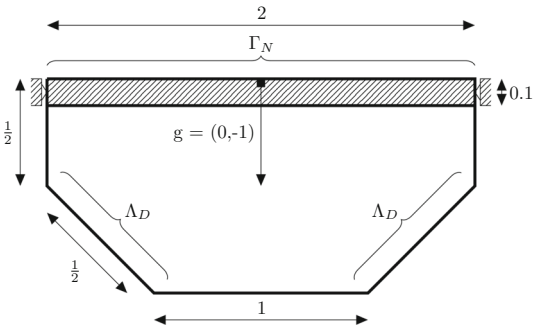

Fig. 9 Setting of the 2d bridge test-case of Sect. 5.3.1; the dashed rectangle corresponds to the deck of the bridge, which is a non-optimizable area of Ω

and η is a small parameter so that the void region $D \setminus \overline{\Omega}$ is filled with a very soft material instead of void (typically, we take $\eta = 10^{-3}$). In this section the Lamé parameters are still given by (5.6) but using $E = 1$, $\nu = 0.3$.

As far as the representation of the optimized part Γ_D of $\partial\Omega$ is considered, it is constrained to belong to a planar subset Λ_D of the boundary ∂D in the examples of Sects. 5.3.1 and 5.3.2. In this case, it is represented by means of a level set function on a subset of the real line. In Sect. 5.3.3, the set Λ_D is a whole region of D. Then, Γ_D is represented by means of a different level set function $\psi : \Lambda_D \to \mathbb{R}$ from that ϕ used to represent Ω. Both cases are simple adaptations from the general idea outlined in Sect. 5.2.2; see also [56,57] about this type of representation.

The same process as before is applied to approximate the transition region Σ_D between homogeneous Dirichlet and Neumann boundary condition in the formulation of Problem (5.13), and we do not repeat the details for brevity.

5.3.1 Optimization of the shape of a two-dimensional bridge and its supports

We first consider the joint optimization of the shape of a two-dimensional bridge Ω and of the location of its fixations. The situation is that depicted in Fig. 9: Ω is enclosed inside a two-dimensional computational domain D meshed with 80537 triangles; a unit vertical load is distributed along the upper deck Γ_N, a neighborhood of which is imposed to be part of Ω. We optimize Ω and the set of fixations Γ_D (which is restrained to a subset Λ_D of the lower part of ∂D) with respect to the elastic compliance of the configuration; more precisely, the optimization problem reads as (5.13) with the expressions:

$$j(u) = \int_{\Gamma_N} g \cdot u \, ds, \quad \ell_V = 50, \quad \ell_D = 10.$$

We perform two optimization experiments, corresponding to different initial states as for Ω and Γ_D; the results are reported in Fig. 10 and Fig. 11. In particular, we observe very different optimized topologies depending on the initial definition of the fixation region Γ_D.

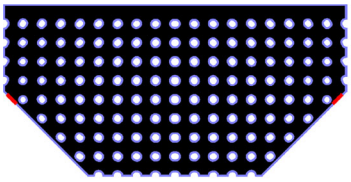

(a) *Iteration 1*

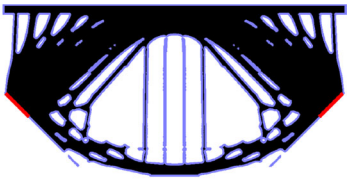

(b) *Iteration 25*

(c) *Iteration 100*

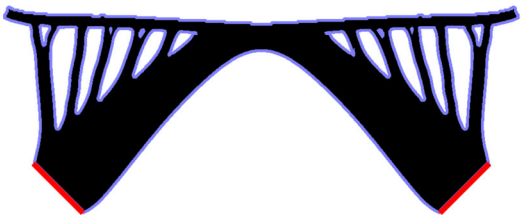

(d) *Deformed configuration of the optimized shape*

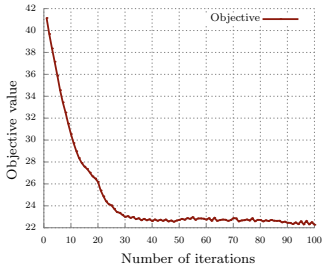

(e) *Convergence history*

Fig. 10 Concurrent optimization of the shape and the fixation regions of the bridge of Sect. 5.3.1, with an initial configuration for Γ_D composed of two line segments

5.3.2 Optimization of the shape of a force inverter and of its fixations

Our second example deals with the optimization of a force inverter mechanism, that is, a device which convert a pulling force into a pushing one. The details of the test-case are presented on Fig. 12: the considered shapes Ω are contained in a box D meshed with 78408 triangles; they are subjected to a given load $g = (-1, 0)$ applied on a non optimizable subset Γ_N of their left-hand side, and they are attached on another subset Γ_D of $\partial\Omega$, contained in the upper and lower sides of ∂D. In this context, the aim is to optimize the overall shape Ω and the location of the fixations Γ_D so that the elastic displacement of Ω on a non optimizable subset Γ_T is maximized. The symmetry of the optimized shapes with respect to the horizontal axis is enforced.

More precisely, in the general formulation of the problem (5.13), we set:

$$j(u) = 10^{-1} \int_{\Gamma_T} |u - (1,0)|^2 \, ds - 10^{-3} \int_{\Gamma_N} u_1 \, ds, \quad \ell_V = 5 \times 10^{-3}, \quad \ell_D = 0$$

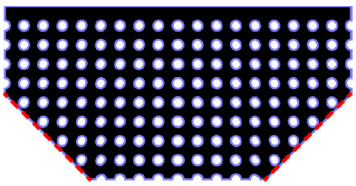

(a) *Iteration 1*

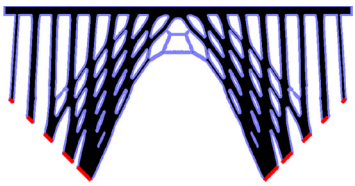

(b) *Iteration 25*

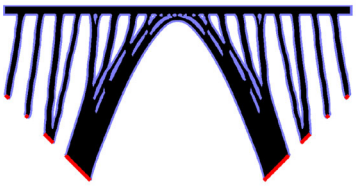

(c) *Iteration 100*

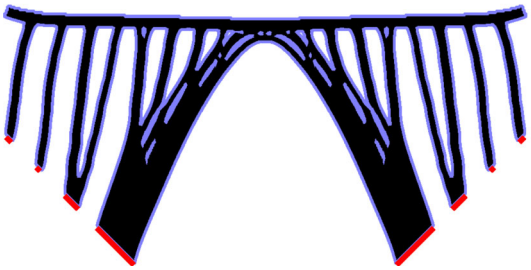

(d) *Deformed configuration of the optimized shape*

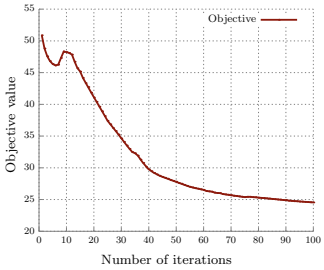

(e) *Convergence history*

Fig. 11 Concurrent optimization of the shape and the fixation regions of the bridge of Sect. 5.3.1, with an initial configuration for Γ_D composed of 18 line segments

where the little penalization on the compliance was added to make it easier to obtain a connected structure. The results associated to two different initializations are presented on Figs. 13 and 14.

5.3.3 Optimization of the shape and the support regions of a two-dimensional cantilever beam

Our last example deals with the concurrent optimization of the shape of a classical 2d cantilever beam and its fixation zones. The considered shapes Ω are contained in a fixed computational domain D, meshed with 39402 triangles. They are attached on the upper and lower left corners, as well as on a region Γ_D which is subjected to optimization, and which is constrained to be contained inside a given region $\mathcal{D}_D \subset D$. A vertical load $g = (0, -1)$ is applied on a non optimizable subset Γ_N of the right-hand boundary; see Fig. 15. Notice that, contrary to the previous two examples, the region Γ_D is not a subset of a region $\Lambda_D \subset \partial\mathcal{D}$ but it is allowed to evolve freely inside

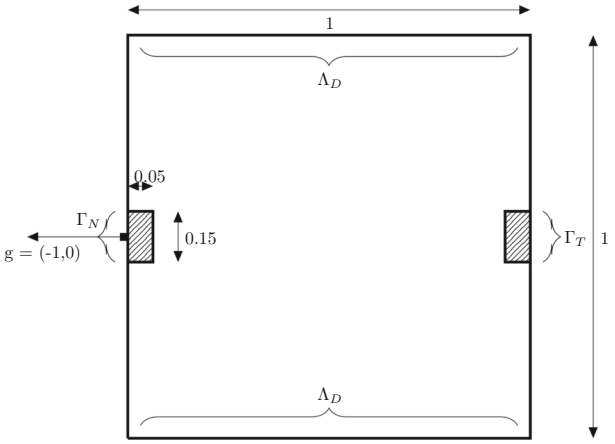

Fig. 12 Setting of the force inverter test-case of Sect. 5.3.2. The two dashed rectangles represent non optimizable areas

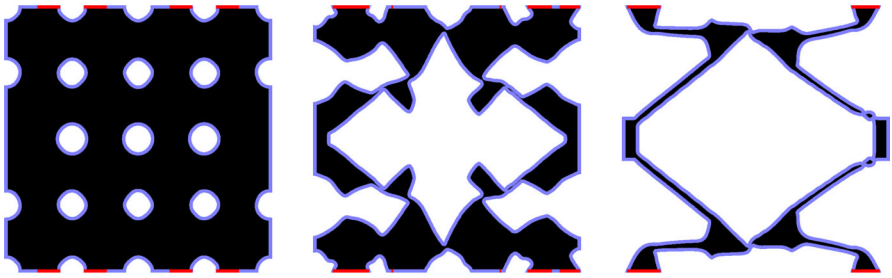

(a) *Iteration 1* **(b)** *Iteration 50* **(c)** *Iteration 100*

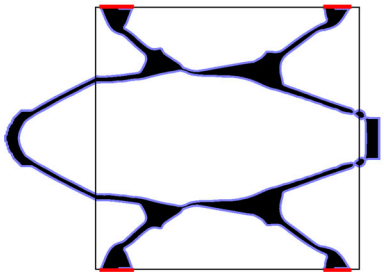

(d) *Deformed configuration of the optimized shape*

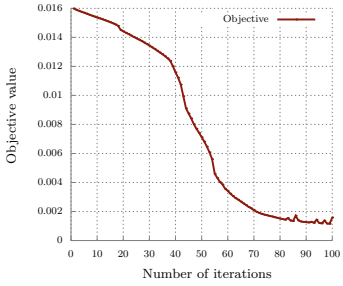

(e) *Convergence history*

Fig. 13 Concurrent optimization of the shape and the fixation regions of the force inverter of Sect. 5.3.2, with an initial configuration for Γ_D composed of 8 line segments

(a) *Iteration 1* **(b)** *Iteration 50* **(c)** *Iteration 300*

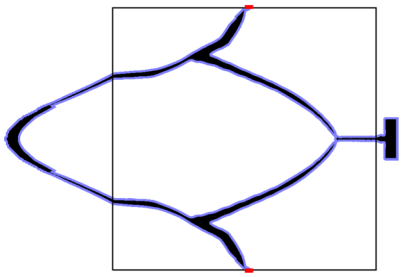

(d) *Deformed configuration of the optimized shape*

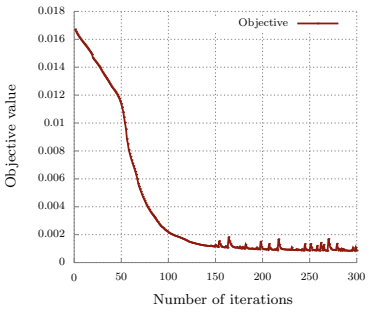

(e) *Convergence history*

Fig. 14 Concurrent optimization of the shape and the fixation regions of the force inverter of Sect. 5.3.2, with an initial configuration for Γ_D composed of 4 line segments

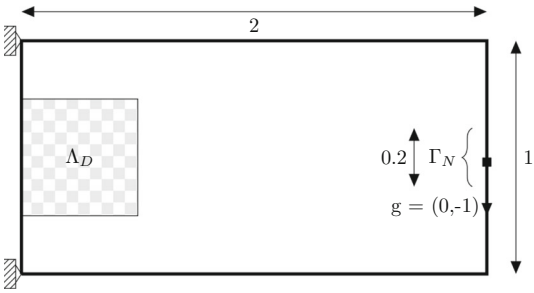

Fig. 15 Setting of the 2d cantilever test-case of Sect. 5.3.3

a region of $\mathcal{D}$. This demands a little adaptation of the framework described above (another level set function is used to identify the region Γ_D).

Symmetry with respect to the horizontal axis is imposed on the optimized shape.

All things considered, we consider the optimization problem (5.13) with the expressions:

$$j(u) = \int_{\Gamma_T} g \cdot u \, ds, \quad \ell_V = 150, \quad \ell_D = 0.$$

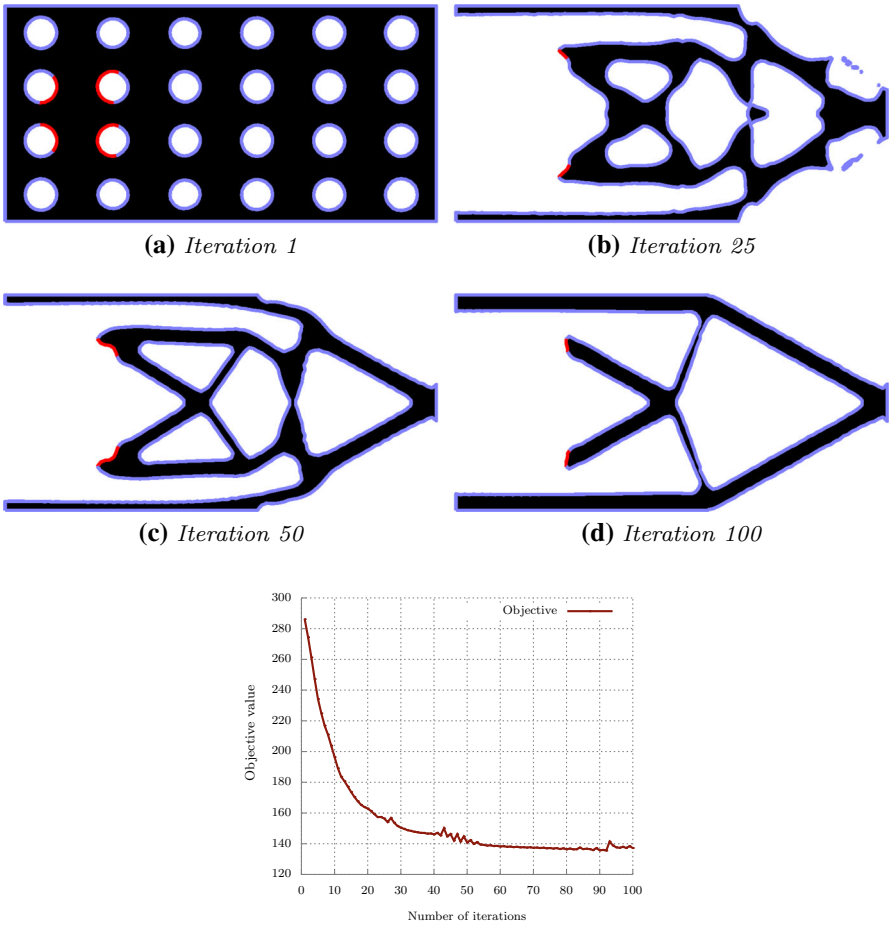

(a) *Iteration 1* **(b)** *Iteration 25*

(c) *Iteration 50* **(d)** *Iteration 100*

(e) *Convergence graph*

Fig. 16 Concurrent optimization of the shape Ω and the fixation zones Γ_D of the two-dimensional cantilever of Sect. 5.3.3 (the latter are represented using red lines) (color figure online)

Results are presented on Fig. 16; obviously, the Dirichlet region aims to get as close as possible to the application region of the load g. It also tends to concentrate on the top and bottom corners of the region $\mathcal{D}_D$, following insofar as possible the principal stress directions of the structure.

6 Conclusions and perspectives

In this article, we have considered the optimization problem of a shape Ω and of the regions of its boundary supporting different types of boundary conditions in the description of the underlying physical context. Relying on the basic model of a Laplace equation, we have calculated the shape derivative of a quite general objective func-

tion $J(\Omega)$ with respect to variations of the 'inhomogeneous Neumann–homogeneous Neumann' and 'homogeneous Dirichlet–homogeneous Neumann' transition zones Σ_N and Σ_D. Since the second expression is very difficult to use in practice, for it involves a measure of the 'singular' character of the Laplace equation near Σ_D, we have proposed an approximation process to carry out this optimization in practice, which consists in 'smearing' the sharp transition Σ_D between homogeneous Dirichlet and homogeneous Neumann boundary conditions into a band with small thickness ε supporting Robin-like boundary conditions. We have verified the numerical efficiency of this process on several application examples involving notably the context of linearized elastic structures in two or three space dimensions. In these examples, we have made the simplifying assumption that Σ_D belongs to a 'flat' region, and it would be interesting to also conduct the optimization in the case where it is enclosed in a curved surface. Although this setting is already dealt with in our theoretical developments, this is a little more demanding from the numerical point of view: in particular, we would have to apply the level set method on a curved surface, which could for instance involve the so-called 'closest point method'; see for instance [42]. Also, it would be natural and interesting to extend the idea approximate 'singular' transition regions between different types of boundary conditions to different physics than those considered in this article (e.g. electromagnetism); let us again mention that it was already used in [24] in the context of the acoustic Helmholtz equations.

Acknowledgements The authors were partially supported by the ANR Shapo grant. They warmly thank A. Glière and K. Hassan from CEA-LETI, as well as G. Michailidis for fruitful discussions at the origin of this work. The third author gratefully acknowledges the support of the ANR through the project GEOMETRYA, the project COMEDIC and the LabEx PERSYVAL-Lab (ANR-11-LABX-0025-01).

A Some facts from tangential calculus

In this section, we briefly review some facts from tangential calculus which come in handy in several parts of this article; see [33] for a more exhaustive presentation.

Let Ω be a smooth bounded domain in $\mathbb{R}^d$. There exists a tubular neighborhood U of its boundary $\partial\Omega$ such that the projection mapping $p_{\partial\Omega} : U \to \Gamma$ given by

$$p_{\partial\Omega}(y) = \text{the unique } x \in \Gamma \text{ s.t. } |x - y| = d(y, \Gamma)$$

is well-defined and smooth; see [7], Th. 3.1. This allows to define smooth extensions of the normal vector field n and of any tangential vector field $\tau : \partial\Omega \to \mathbb{R}^d$ to U via the formulas:

$$n(y) \equiv n(p_{\partial\Omega}(y)), \text{ and } \tau(y) \equiv \tau(p_{\partial\Omega}(y)),$$

respectively. From these notions, we define the mean curvature κ of $\partial\Omega$ by

$$\kappa = \mathrm{div} n. \tag{A.1}$$

In this context, the *tangential gradient* $\nabla_{\partial\Omega} f$ of a smooth enough function $f : \partial\Omega \to \mathbb{R}$ is defined by $\nabla_{\partial\Omega} f = \nabla \widetilde{f} - (\nabla \widetilde{f} \cdot n)n$, where $\widetilde{f}$ is any smooth extension of f to an open neighborhood of $\partial\Omega$.

In the same spirit, the *tangential divergence* $\mathrm{div}_{\partial\Omega} V$ of a smooth vector field $V : \partial\Omega \to \mathbb{R}^d$ is defined by $\mathrm{div}_{\partial\Omega} V := \mathrm{div}\widetilde{V} - (\nabla \widetilde{V} n) \cdot n$, where $\widetilde{V}$ is any extension of V to an open neighborhood of $\partial\Omega$.

Let us finally recall the following integration by parts formulas on the boundary of smooth domains; see [33], Prop. 5.4.9 for the first point, and [19], §5.5.4 for the second one.

Proposition 7 *Let $\Omega \subset \mathbb{R}^d$ be a smooth bounded domain with boundary $\partial\Omega$;*

1. *Let $u \in H^1(\partial\Omega)$ and $V \in H^1(\partial\Omega)^d$; then:*

$$\int_{\partial\Omega} div_{\partial\Omega} V u \, ds = \int_{\partial\Omega} (-V \cdot \nabla_{\partial\Omega} u + \kappa u V \cdot n) \, ds$$

2. *Let G be a subset of $\partial\Omega$ with smooth boundary Σ, and denote by n_Σ its unit normal vector pointing outward G (n_Σ is a tangent vector field to $\partial\Omega$). Let $u \in H^1(\partial\Omega)$ and $V \in H^1(\partial\Omega)^d$; then:*

$$\int_G div_{\partial\Omega} V \, u \, ds = \int_\Sigma uV \cdot n_\Sigma d\ell + \int_G (-\nabla_{\partial\Omega} u \cdot V + \kappa u V \cdot n) \, ds,$$

where $d\ell$ denotes integration over the codimension 2 submanifold Σ of $\mathbb{R}^d$.

References

1. Adams, R.A., Fournier, J.J.: Sobolev Spaces, vol. 140. Academic Press, Cambridge (2003)
2. Agmon, S., Douglis, A., Nirenberg, L.: Estimates near the boundary for solutions of elliptic partial differential equations satisfying general boundary conditions. I. Commun. Pure Appl. Math. **12**, 623–727 (1959)
3. Allaire, G.: Shape Optimization by the Homogenization Method, vol. 146. Springer, Berlin (2001)
4. Allaire, G., Dapogny, C., Delgado, G., Michailidis, G.: Multi-phase structural optimization via a level set method. ESAIM: Control Optim. Calculus Var. **20**, 576–611 (2014)
5. Allaire, G., Jouve, F., Toader, A.-M.: Structural optimization using sensitivity analysis and a level-set method. J. Comput. Phys. **194**, 363–393 (2004)
6. Allaire, G., Schoenauer, M.: Conception optimale de structures, vol. 58. Springer, Berlin (2007)
7. Ambrosio, L., Soner, H.M.: Level set approach to mean curvature flow in arbitrary codimension. J. Differ. Geom. **43**, 693–737 (1994)
8. Azegami, H., Ohtsuka, K., Kimura, M.: Shape derivative of cost function for singular point: evaluation by the generalized J integral. JSIAM Lett. **6**, 29–32 (2014)
9. Babuška, I., Suri, M.: The p-and hp versions of the finite element method, an overview. Comput. Methods Appl. Mech. Eng. **80**, 5–26 (1990)
10. Barone, M., Caulk, D.: Optimal arrangement of holes in a two-dimensional heat conductor by a special boundary integral method. Int. J. Numer. Methods Eng. **18**, 675–685 (1982)
11. Bawa, H.: Manufacturing Processes-II, vol. 2. Tata McGraw-Hill Education, New York (2004)
12. Bendsoe, M.P., Sigmund, O.: Topology Optimization: Theory, Methods, and Applications. Springer, Berlin (2013)
13. Brezis, H.: Functional Analysis. Sobolev Spaces and Partial Differential Equations. Springer, Berlin (2010)

14. Burger, M.: A framework for the construction of level set methods for shape optimization and reconstruction. Interfaces Free Bound. **5**, 301–329 (2003)
15. Céa, J.: Conception optimale ou identification de formes, calcul rapide de la dérivée directionnelle de la fonction coût, ESAIM: Mathematical Modelling and Numerical Analysis, 20, pp. 371–402 (1986)
16. Costabel, M.: Boundary integral operators on lipschitz domains: elementary results. SIAM J. Math. Anal. **19**, 613–626 (1988)
17. Costabel, M., Dauge, M.: A singularly mixed boundary value problem. Commun. Partial Differ. Equ. **21**, 1919–1949 (1996)
18. Costabel, M., Stephan, E.: Curvature terms in the asymptotic expansions for solutions of boundary integral equations on curved polygons. J. Integral Equ. 353–371 (1983)
19. Dapogny, C.: Shape optimization, level set methods on unstructured meshes and mesh evolution. Ph.D. thesis, Paris 6 (2013)
20. Dauge, M.: Elliptic Boundary Value Problems on Corner Domains: Smoothness and Asymptotics of Solutions, vol. 1341. Springer, Berlin (2006)
21. De Gournay, F.: Velocity extension for the level-set method and multiple eigenvalues in shape optimization. SIAM J. Control Optim. **45**, 343–367 (2006)
22. Deaton, J.D., Grandhi, R.V.: A survey of structural and multidisciplinary continuum topology optimization: post 2000. Struct. Multidiscip. Optim. **49**, 1–38 (2014)
23. Delfour, M.C., Zolésio, J.-P.: Shapes and Geometries: Metrics, Analysis, Differential Calculus, and Optimization. SIAM, Philadelphia (2011)
24. Desai, J., Faure, A., Michailidis, G., Parry, G., Estevez, R.: Topology optimization in acoustics and elasto-acoustics via a level-set method. Submitted (2017)
25. Do Carmo, M.P., Flaherty, F.J.: Riemannian Geometry, vol. 115. Birkhäuser, Boston (1992)
26. Dunning, P.D., Kim, H.A.: Introducing the sequential linear programming level-set method for topology optimization. Struct. Multidiscip. Optim. **51**, 631–643 (2015)
27. Elliotis, M., Georgiou, G., Xenophontos, C.: Solving Laplacian problems with boundary singularities: a comparison of a singular function boundary integral method with the p/hp version of the finite element method. Appl. Math. Comput. **169**, 485–499 (2005)
28. Fremiot, G., Sokolowski, J.: Shape sensitivity analysis of problems with singularities. Lecture notes in pure and applied mathematics, pp. 255–276 (2001)
29. Giacomini, M., Pantz, O., Trabelsi, K.: Volumetric expressions of the shape gradient of the compliance in structural shape optimization. arXiv preprint arXiv:1701.05762 (2017)
30. Grisvard, P.: Elliptic Problems in Nonsmooth Domains. SIAM, Philadelphia (2011)
31. Haslinger, J., Makinen, R.A.E.: Introduction to Shape Optimization: Theory, Approximation, and Cmputation, vol. 7. SIAM, Philadelphia (2003)
32. Hecht, F.: New development in freefem++. J. Numer. Math. **20**, 251–265 (2012)
33. Henrot, A., Pierre, M.: Variation et optimisation de formes: une analyse géométrique, vol. 48. Springer, Berlin (2006)
34. Henrot, A., Sokołowski, J.: Mathematical challenges in shape optimization. Control Cybern. **34**, 37–57 (2005)
35. Hiptmair, R., Paganini, A., Sargheini, S.: Comparison of approximate shape gradients. BIT Numer. Math. **55**, 459–485 (2015)
36. Kaya, N.: Machining fixture locating and clamping position optimization using genetic algorithms. Comput. Ind. **57**, 112–120 (2006)
37. Kozlov, V.A., Mazia, V., Rossmann, J.: Elliptic Boundary Value Problems in Domains with Point Singularities, vol. 52. American Mathematical Society, Providence (1997)
38. Lang, S.: Fundamentals of Differential Geometry, vol. 191. Springer, Berlin (2012)
39. Li, Z.-C., Lu, T.-T.: Singularities and treatments of elliptic boundary value problems. Math. Comput. Model. **31**, 97–145 (2000)
40. Lions, J.-L., Magenes, E.: Problèmes aux limites non homogènes et applications. volume i (1968)
41. Ma, J., Wang, M.Y., Zhu, X.: Compliant fixture layout design using topology optimization method. In: 2011 IEEE International Conference on Robotics and Automation (ICRA). IEEE, pp. 3757–3763 (2011)
42. Macdonald, C.B., Ruuth, S.J.: Level set equations on surfaces via the closest point method. J. Sci. Comput. **35**, 219–240 (2008)
43. Marigo, J.-J.: Plasticité et rupture (2016)

44. McLean, W.C.H.: Strongly Elliptic Systems and Boundary Integral Equations. Cambridge University Press, Cambridge (2000)
45. Mohammadi, B., Pironneau, O.: Applied Shape Optimization for Fluids. Oxford University Press, Oxford (2010)
46. Murat, F., Simon, J.: Sur le contrôle par un domaine géométrique, Preprint of the Laboratoire d'Analyse Numérique (76015), p. 222 (1976)
47. Ohtsuka, K.: Shape optimization by generalized j-integral in Poisson's equation with a mixed boundary condition. In: International Conference Continuum Mechanics Focusing on Singularities. Springer, pp. 73–83 (2016)
48. Osher, S., Sethian, J.A.: Fronts propagating with curvature-dependent speed: algorithms based on Hamilton–Jacobi formulations. J. Comput. Phys. **79**, 12–49 (1988)
49. Rakotondrainibe, L.: Modélisation mécanique d'une "Face Accessoire Assemblée" et optimisation d'un modèle simplifié., Ph.D. thesis, Ecole Polytechnique X (2017)
50. Selvakumar, S., Arulshri, K., Padmanaban, K., Sasikumar, K.: Design and optimization of machining fixture layout using ANN and DOE. Int. J. Adv. Manuf. Technol. **65**, 1573–1586 (2013)
51. Sethian, J.A.: Level Set Methods and Fast Marching Methods: Evolving Interfaces in Computational Geometry, Fluid Mechanics, Computer Vision, and Materials Science, vol. 3. Cambridge University Press, Cambridge (1999)
52. Sethian, J.A., Wiegmann, A.: Structural boundary design via level set and immersed interface methods. J. Comput. Phys. **163**, 489–528 (2000)
53. Sokolowski, J., Zolesio, J.-P.: Introduction to Shape Optimization. Springer, Berlin (1992)
54. Subbarao, R., Meer, P.: Nonlinear mean shift over Riemannian manifolds. Int. J. Comput. Vis. **84**, 1–20 (2009)
55. Wang, M.Y., Wang, X., Guo, D.: A level set method for structural topology optimization. Comput. Methods Appl. Mech. Eng. **192**, 227–246 (2003)
56. Xia, Q., Shi, T.: Topology optimization of compliant mechanism and its support through a level set method. Comput. Methods Appl. Mech. Eng. **305**, 359–375 (2016)
57. Xia, Q., Wang, M.Y., Shi, T.: A level set method for shape and topology optimization of both structure and support of continuum structures. Comput. Methods Appl. Mech. Eng. **272**, 340–353 (2014)
58. Zhang, W., Zhao, L., Cai, S.: Shape optimization of dirichlet boundaries based on weighted b-spline finite cell method and level-set function. Comput. Methods Appl. Mech. Eng. **294**, 359–383 (2015)

Affiliations

Charles Dapogny[1] · Nicolas Lebbe[2] · Edouard Oudet[1]

✉ Charles Dapogny
charles.dapogny@univ-grenoble-alpes.fr

Nicolas Lebbe
Nicolas.LEBBE@cea.fr

Edouard Oudet
edouard.oudet@univ-grenoble-alpes.fr

[1] CNRS, Grenoble INP, LJK, Univ. Grenoble Alpes, 38000 Grenoble, France

[2] CEA, LETI, Univ. Grenoble Alpes, 38000 Grenoble, France